JACS
JOURNAL OF THE AMERICAN CHEMICAL SOCIETY
Article
pubs.acs.org/JACS

Why Does Alkylation of the N−H Functionality within M/NH Bifunctional Noyori-Type Catalysts Lead to Turnover?

Pavel A. Dub,*[,∥] Brian L. Scott,[‡] and John C. Gordon*[,∥]

[∥]Chemistry Division, and [‡]Materials and Physics Applications Division, Los Alamos National Laboratory, Los Alamos, New Mexico 87545, United States

Supporting Information

ABSTRACT: Molecular metal/NH bifunctional Noyori-type catalysts are remarkable in that they are among the most efficient artificial catalysts developed to date for the hydrogenation of carbonyl functionalities (loadings up to ~10^{-5} mol %). In addition, these catalysts typically exhibit high C═O/C═C chemo- and enantioselectivities. This unique set of properties is traditionally associated with the operation of an unconventional mechanism for homogeneous catalysts in which the chelating ligand plays a key role in facilitating the catalytic reaction and enabling the aforementioned selectivities by delivering/accepting a proton (H^+) via its N−H bond cleavage/formation. A recently revised mechanism of the Noyori hydrogenation reaction (Dub, P. A. et al. *J. Am. Chem. Soc.* **2014**, *136*, 3505) suggests that the N−H bond is not cleaved but serves to stabilize the turnover-determining transition states (TDTSs) via strong N−H···O hydrogen-bonding interactions (HBIs). The present paper shows that this is consistent with the largely ignored experimental fact that alkylation of the N−H functionality within M/NH bifunctional Noyori-type catalysts leads to detrimental catalytic activity. The purpose of this work is to demonstrate that decreasing the strength of this HBI, ultimately to the limit of its complete absence, are conditions under which the same alkylation may lead to beneficial catalytic activity.

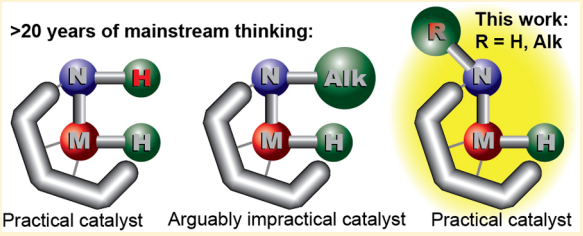

1. INTRODUCTION

Catalytic hydrogenations represent the largest-volume human-made chemical reactions in the world.[1] Many industrially important processes are based on a homogeneous version of this reaction.[2] Single-phase catalysis indeed affords a number of convenient properties such as mild reaction conditions, low cost, operational simplicity, and high activities and selectivities that can be tuned via electronic and steric effects of the ligands, ease of catalyst structure determination, and reaction mechanism analysis that can also be readily probed. Among three functional groups (C═O, C═N, C═C), special attention is given to the hydrogenation of carbonyl functionalities,[3] with ketones being among the most common substrates.[4] Before 1995, the vast majority of reported homogeneous transition metal catalysts were hydrogenating ketonic substrates with relatively low turnover efficiencies (TEs)[5] (catalyst loadings of ~1 mol %, high temperatures and/or long reaction times) and low C═O/C═C chemoselectivities. These catalysts are believed to operate via a classical Schrock−Osborn (inner-sphere) mechanism[6] now distinguished as a "monohydride" and a "dihydride" version as outlined in Scheme 1.[7] Details have been explained elsewhere.[7,8]

An example of a catalyst that is proposed to operate via the classical Schrock−Osborn mechanism is shown in Scheme 2.[9]

The Ir (pre)catalyst complex is initially coordinatively unsaturated (16e$^-$) and, in addition, contains a labile η^4-cyclooctadiene ligand which is typically expected to leave the

Scheme 1. Classical Schrock−Osborn (Inner-Sphere) Mechanism for the Hydrogenation of Ketonic Substrates with Molecular Catalysts

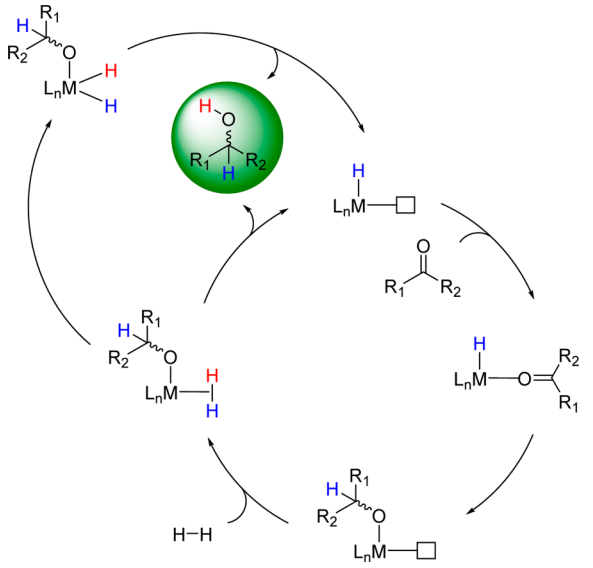

Received: November 10, 2016
Published: January 3, 2017

DOI: 10.1021/jacs.6b11666
J. Am. Chem. Soc. 2017, 139, 1245−1260

Scheme 2. An Example of a Catalyst That Is Proposed To Operate via the Classical Schrock–Osborn Mechanism[9]

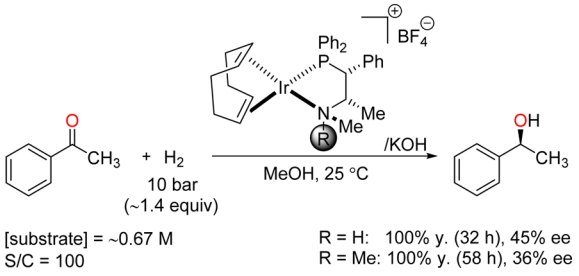

coordination sphere of the metal (via decoordination and/or ultimately hydrogenation into cyclooctane)[10] during the catalytic reaction, providing more coordination vacancies. Low TEs, H/D labeling experiments, and other observations such as methylation of the N–H functionality within the chelating PN ligand that results in a small impact on the TE are arguably consistent with the operation of the inner-sphere mechanism initially proposed by Dahlenburg.[9]

In 1995, Noyori, Ikariya and co-workers discovered a novel and very unusual catalyst for the hydrogenation of ketonic substrates.[11] The catalyst, the key structural parameter of which is an N–H functionality, was different from previously described examples in several aspects: extremely high TEs (loadings of $\sim 10^{-4}$ mol %, ambient temperatures and/or short reaction times) and high C=O/C=C chemoselectivities.[4,11] This remarkable and unique set of observed properties was further attributed to the operation of a novel, nonclassical mechanism, within which the ketonic substrate is reduced in the outer-sphere via a six-membered pericyclic transition state $\mathbf{TS_a}$ and the H–H bond is then cleaved to regenerate the catalyst via direct $\mathbf{TS_b}$ or solvent-assisted $\mathbf{TS_c}$ metal–ligand cooperation, Scheme 3.[4,12] Details have been explained elsewhere.[4,12,13]

This new mechanism not only realized the origin of unprecedently high rates and high C=O/C=C chemoselectivities but also was consistent with a very notable experimental observation, the so-called "N–H effect". The latter is manifested in the methylation of the N–H functionality which led to a totally inactive catalyst.[4] The discovery of the Noyori catalyst stimulated the development of a powerful field which became known as M/NH bifunctional catalysis.[16] Hundreds of new ligands and catalysts, the key structural parameter of which is traditionally prescribed as a "deprotonatable" N–H functionality, were developed and synthesized for the hydrogenation of carbonyl functionalities over the past decade.[17] As a result, these catalysts have arguably become the most efficient molecular catalysts for the hydrogenation of ketones,[18] carboxylic and carbonic acid derivatives,[19] and its microscopic[20] reverse corresponding to dehydrogenation.[21]

In describing mechanisms with M/NH bifunctional Noyori-type catalysts, the conventional Noyori mechanism (Scheme 3)[22] remained in mainstream thinking for over 15 years.[23] There are two principal reasons for this. First, the concepts of the so-called metal–ligand bifunctional mechanism (MLBM) and metal–ligand cooperation (MLC) manifested in $\mathbf{TS_a}$ and $\mathbf{TS_b}$–$\mathbf{TS_c}$ in Scheme 3, respectively, gained broad support from the classical organometallic chemist's mechanistic toolbox, i.e. stoichiometric NMR experiments, kinetics studies including H/D labeling, and gas-phase computations.[23,24] A critical overview of these methods used to study catalytic reactions is available

Scheme 3. Nonclassical Noyori (Outer-Sphere) Mechanism for the Hydrogenation of Ketonic Substrates with M/NH Bifunctional Noyori-Type Catalysts (The Ligand Plays a Key Role in Facilitating the Process by Delivering/Accepting a H^+)

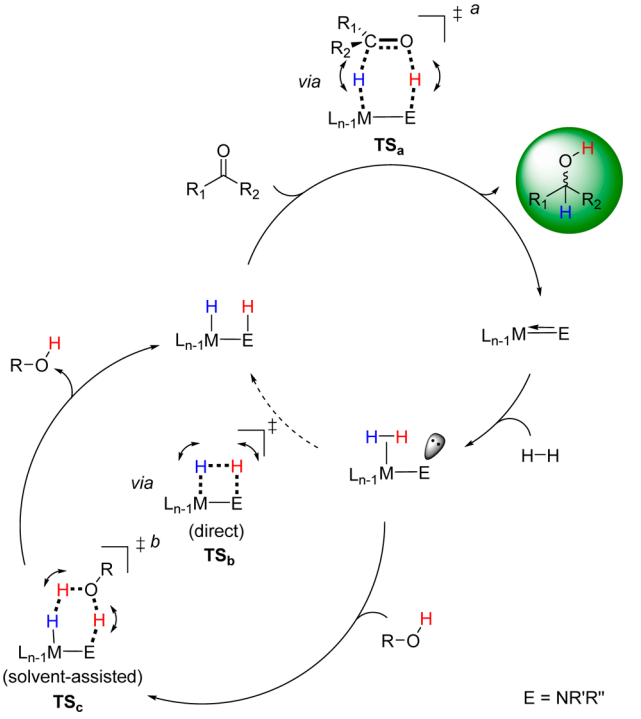

[a]Sometimes, particularly in recent years, represented as a stepwise process, i.e., consecutive transfer of H^- and H^+ equivalents via an ion-pair intermediate even in gas-phase computations.[14] [b]>10 kcal·mol^{-1} more favorable than $\mathbf{TS_b}$ in gas-phase computations.[15]

elsewhere.[18] Second, numerous reports from 1995 to 2015 have supported the "most convincing" experimental observation; various attempts to methylate, or more, generally, alkylate an N–H functionality, resulted in a dramatic drop in catalytic activity, Figure 1.

Catalytic reactions span those of ketones,[4,25] epoxides,[26] esters,[27] carbonates,[28] nitrile hydrogenations,[29] (asymmetric) transfer hydrogenation of ketones[30] or imines,[30c] oxidative lactonization,[31] dehydrogenative oxidation of alcohols using O_2,[32] and dehydrogenation of formic acid.[33] To the best of our knowledge, it has never been questioned[30b] why in selected cases of N–H alkylated, coordinatively saturated (18e$^-$)[34] (pre)catalysts, catalytic activity was either zero or, as a matter of fact, in some cases reached a few % detectable conversion (~5%), the extent of which also depended on the nature of the substrate. No attempt was ever made to explain this activity, as well as how its existence is related to the conventional Noyori mechanism.[22] In contrast, these "drops in activity" were generally taken as confirmatory evidence of the participation of the ligand in the catalytic reaction via a reversible H^+ transfer through concerted $\mathbf{TS_a}$–$\mathbf{TS_c}$ in Figure 1 (or less frequently, via a stepwise analog of $\mathbf{TS_a}$).[17,23]

Recently, the identity of the conventional Noyori mechanism[22] as the *bona fide* reaction path operable in ketone reductions with the pioneering prototypes of bifunctional catalysts was disputed,[35] both via computational chemistry using full catalyst models and including solvent effects and by careful reconsideration of available experimental data. First, it

DOI: 10.1021/jacs.6b11666
J. Am. Chem. Soc. 2017, 139, 1245–1260

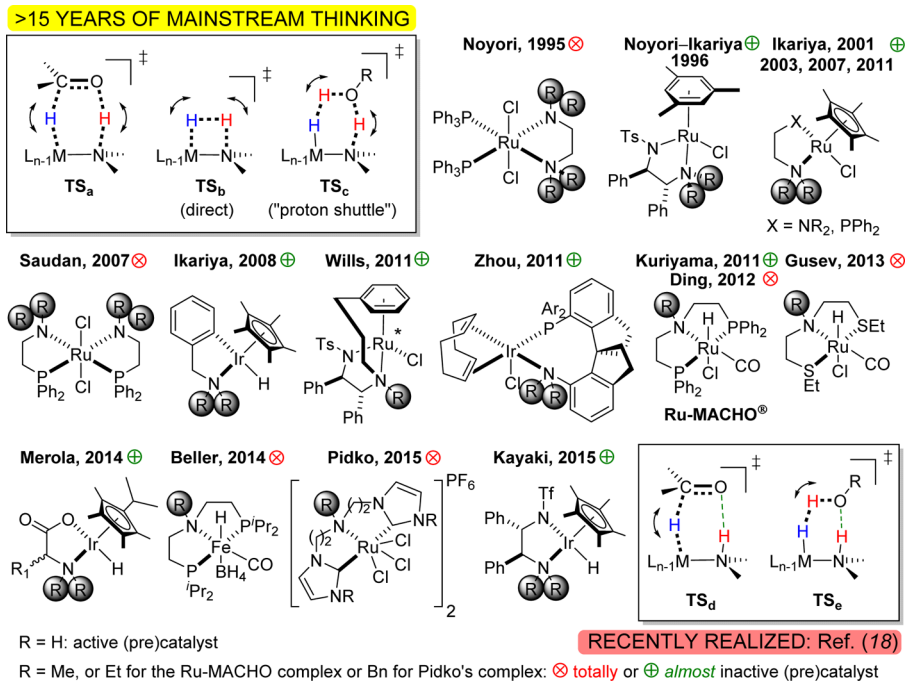

Figure 1. Representative examples of *in situ* generated or well-defined, isolable M/NH Noyori-type bifunctional (pre)catalysts in which NH/NAlk substitution leads to complete catalyst deactivation or very small catalytic activities. *Inversion of metal absolute configuration upon alkylation (X-ray). For more details on the role of TS_a–TS_e, see ref 18.

was realized that the concerted transition states TS_a and TS_c have no mechanistic relevance in solution,[35,36] whereas cleavage of the H–H bond via TS_b is energetically unfeasible in the catalytic reaction, unless a quantum tunneling effect is involved.[18] Second, this realization (through identification of new reaction intermediates) brought an understanding that not only a new alternative reaction path (due to crossover of pathways) is possible, but also it is actually *energetically more favorable* than the conventional Noyori mechanism[22] for bifunctional catalysts.[18] In particular, a revised mechanism for the Noyori hydrogenation reaction,[35a] also proposed for the Ru-MACHO catalyst,[37] suggests that that the N–H bond is not cleaved, but instead serves to stabilize the turnover-determining transition states (TDTSs)[38] TS_d/TS_e (corresponding to substrate reduction and H–H bond cleavage, respectively) in Figure 1 via strong N–H···O hydrogen-bonding interactions (HBIs). This new reaction path for M/NH bifunctional Noyori-type catalysts was denoted as a H^-/H^+ outer-sphere hydrogenation mechanism (H^-/H^+ OSHM), Scheme 4.[18] Details have been explained elsewhere.[18]

The reaction path within H^-/H^+ OSHM for bifunctional catalysts is based on a *cooperative* and *chemically innocent* ligand.[18] *Cooperation* is manifested in the stabilization of rate-determining TS_d- and/or TS_e-type transition states via relatively strong N–H···O HBIs. *Chemical innocence* implies that the ligand remains chemically intact, i.e. in particular, does not participate in the reaction by delivering/accepting a H^+. The source of the H^+ that neutralizes the anion generated through TS_d, i.e. the anion of the not yet formed reaction product, is either the η^2-H_2 ligand obtained in the following step or a protic solvent molecule, if one is used. This enables catalytic cycles I and II, respectively, as shown in Scheme 4. In protic solvents, catalytic cycle I is usually the dominant one (especially in highly basic media).[35a,37] In aprotic solvents,

Scheme 4. H^-/H^+ Outer-Sphere Hydrogenation Mechanism (H^-/H^+ OSHM) for the Hydrogenation of Ketonic Substrates with M/NH Bifunctional Noyori-Type Catalysts Is Based on a *Cooperative* and *Chemically Innocent* Ligand[18]

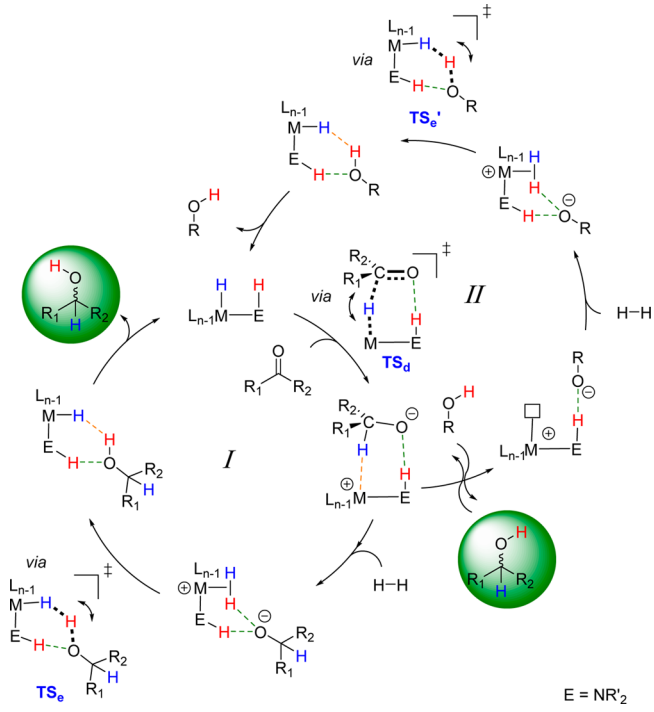

catalytic cycle II fully degenerates into catalytic cycle I and more examples will be described soon.[39]

If we now assume, in contrast to the mainstream thinking of 15 years, that the M/NH bifunctional Noyori-type catalysts shown in Figure 1 do not actually operate via the conventional

DOI: 10.1021/jacs.6b11666
J. Am. Chem. Soc. 2017, 139, 1245–1260

Noyori mechanism, but rather via a H^-/H^+ OSHM reaction path, i.e. the ligand is not involved in H^+ transfer in catalytic cycles, then this becomes consistent with the presence of some level of conversion with selected reported alkylated catalysts/substrates, although it is not immediately clear why the outcome is always detrimental to the catalytic activity. This paper attempts to rationalize the origin of this negative activity based on the revised mechanism for the Noyori hydrogenation reaction.[35a] The ultimate goal of this work is to understand whether alkylation of an N−H functionality within M/NH bifunctional Noyori-type catalysts can actually lead to improved activities and, if so, which conditions need to be met.

2. RESULTS AND DISCUSSION

2.1. Effect of N−H Group(s) Alkylation on the Relative Rate of Hydride Transfer. A prototype of the Noyori catalyst qualitatively and rapidly hydrogenates acetophenone at room temperature within a few minutes, Scheme 5 (reaction 1).[4,11] Methylation of all four N−H functionalities within the chelating bidentate NN ligand resulted in a totally inefficient catalyst, Scheme 5 (reaction 1).[4,11]

Scheme 5. Catalytic Reactions Described by Noyori[4,11] and Kuriyama[27b,40]

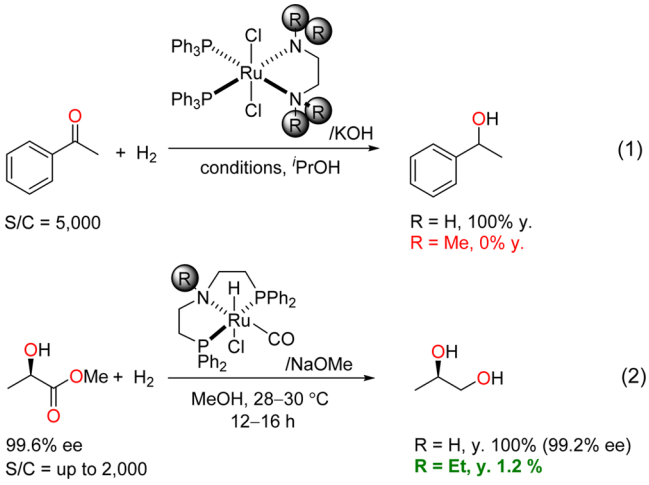

However, when the N−H group now contained within the Ru-MACHO catalyst was replaced by an N−Et fragment, and the substrate used was chiral methyl lactate, the reaction now proceeded with a detectable 1.2% conversion, Scheme 5 (reaction 2).[27b,40] This corresponds to 12 turnovers[5c] after 16 h at 30 °C.[27b] The turnover number (TON)[5c] reaches 55 when the temperature is increased to 80 °C.[27b] What is the origin of these turnovers? One may argue that these arise due to the fact that the catalytic reaction instead proceeds via a classical Schrock−Osborn mechanism. Indeed, partial ligand dissociation within the coordinatively saturated ($18e^-$) *trans*-RuH_2 complex, a key intermediate in the catalytic cycle obtained from Ru-MACHO (pre)catalyst under the reaction conditions,[37] may potentially take place. Such a possibility can in principle explain the origin of a few % conversions for those alkylated catalysts in Figure 1, where it is observed. Although this is imaginable, we do not think this is the case, at least for the vast majority of catalysts shown in Figure 1. First of all, any partial dissociation, even if the polydentate ligand contains a hemilabile auxiliary, is arguably unfavorable from a thermodynamic point of view. Second, even if somehow such a dissociation takes place under reaction conditions,[41] the result of this transformation would not be consistent with extremely high enantioselectivities of ~99% observed for some of these catalysts (e.g., Noyori−Ikariya catalysts).[18] Third, reduction of a carbonyl functionality via an inner-sphere pathway is currently recognized as more energetically difficult than via an outer-sphere pathway.[42] This is why high temperatures and high catalyst loadings (1 mol %) are typically used with these catalysts, even for easy-to-hydrogenate substrates such as ketones. In contrast, the Ru-MACHO catalyst in which an ethyl group, instead of a hydrogen atom is present at N, can hydrogenate the *much less electrophilic* (more difficult-to-hydrogenate) chiral methyl lactate ester with up to 55 turnovers,[27b] which, as a matter of fact, corresponds to an actual catalyst loading of ~2 mol %, assuming complete conversion!

Analyzing available kinetic curves[30c,33] for the alkylated catalysts, we propose that the origin of zero to a few % conversions for alkylated catalyst−substrate combinations in Figure 1 is rather a kinetic phenomenon and that the catalytic reactions with both N−H and N−Alk catalysts proceed through the same reaction path that was recently discovered for the Noyori catalyst.[35a] The revised mechanism of the Noyori hydrogenation reaction that corresponds to the concept of H^-/H^+ OSHM (Scheme 4, catalytic cycle I)[35a] not only well rationalizes the origin of high TEs and C=O/C=C chemoselectivities but also alternatively explains the nature of the "N−H effect": replacing the hydrogen atom with an alkyl group not only will destroy the favorable H-bonding interaction but also decreases the nucleophilicity of the hydride fragment due to a necessarily generated repulsive interaction between the alkyl group within the second coordination sphere of the catalyst and the substrate within the catalyst−substrate complex (CSC) as shown in Figure 2a.[18]

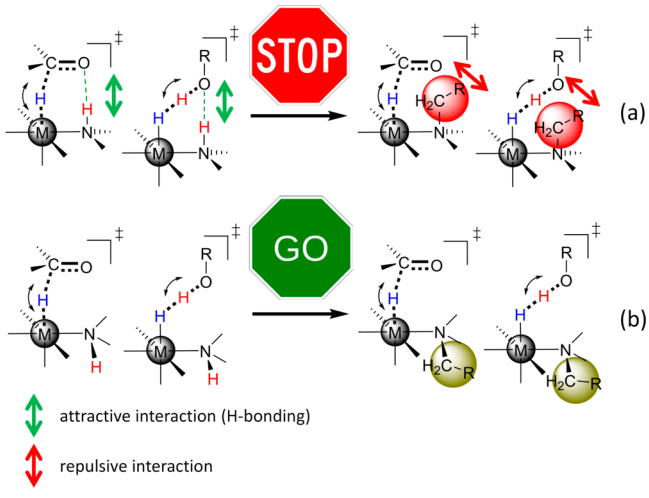

Figure 2. Explanation of the "N−H effect" based on the revised mechanism of the Noyori hydrogenation reaction.[35a]

As a result, any attempt to alkylate an N−H functionality within M/NH Noyori-type catalysts that have planar H−N−M−X dihedral angles (X = H, Cl, etc.) will necessarily lead to a decrease in the outer-sphere hydride transfer rate and arguably, as a result, also in the overall rate of the catalytic reaction.

DOI: 10.1021/jacs.6b11666
J. Am. Chem. Soc. 2017, 139, 1245−1260

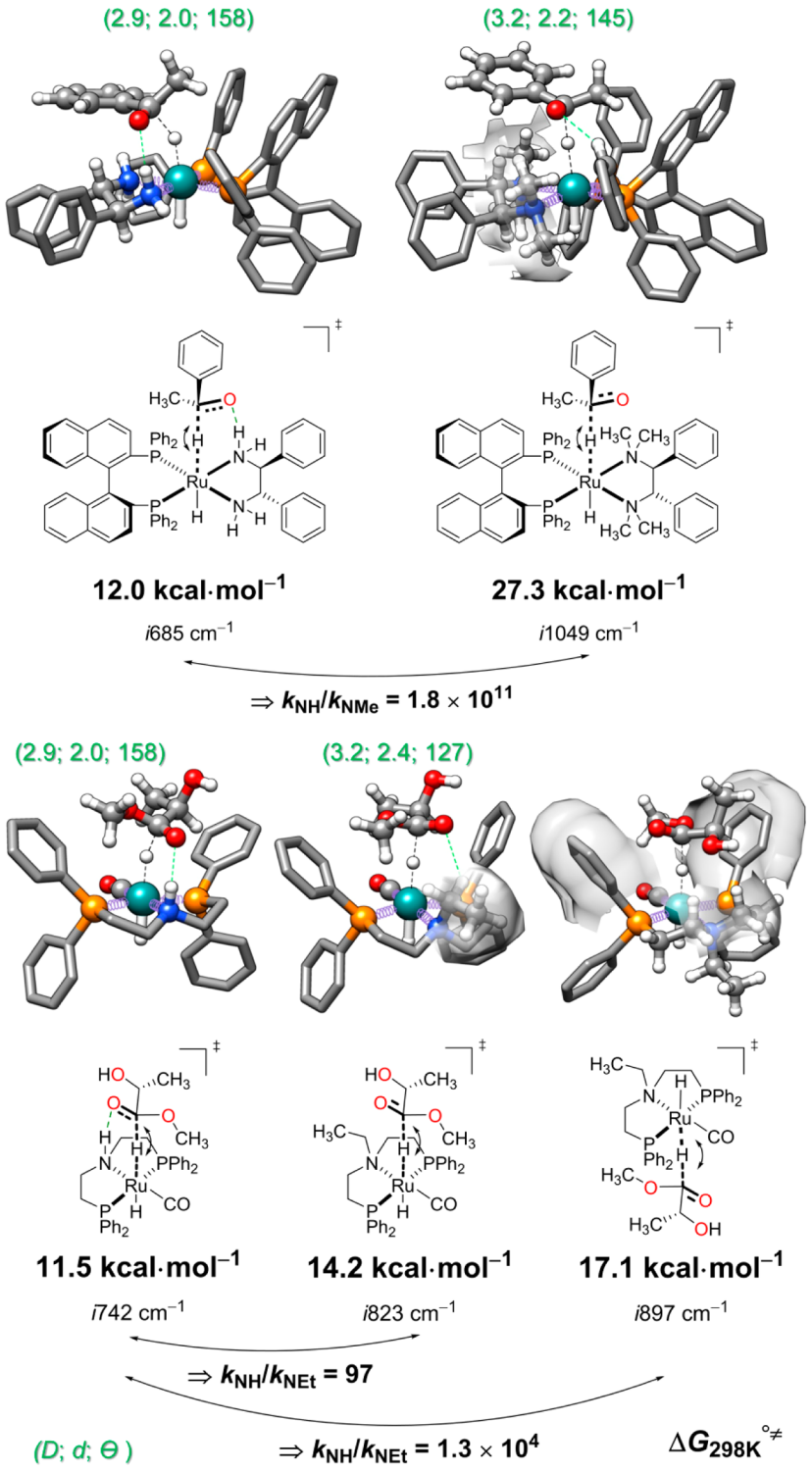

Figure 3. Computed effect of N−H group(s) alkylation on the relative rate of hydride transfer: transition states optimized at the DFT/ωB97X-D/ECP28MDF_VTZ(Ru)/6-311++G**(all others)/SMD(propan-2-ol or methanol) level of theory (in the ball and stick representations, noncritical H atoms are omitted). *D* and *d* are X···O (X = N, C) and H···O lengths in Å. *θ* is the X−H···O angle in deg.

Figure 3 provides the first computational support for this explanation.[43]

Complete methylation of four N−H groups within Noyori's catalyst significantly destabilizes the transition state corresponding to hydride transfer via (a) the absence of any N−H···O HBIs and (b) repulsion within the CSC resulting from the presence of bulky methyl groups within the second coordination sphere of the metal complex, Figure 3.[44] As a result, the activation barrier of hydride transfer increases by 15.3 kcal·mol^{-1} in the case of the fully *N*-methylated complex, which corresponds to a 1.8×10^{11} times decrease of the hydride transfer rate compared to the analogous N−H complex. It is thus not surprising that complete methylation results in a "fully inactive catalyst"[4,11] in this reaction.[45] In the case of the Ru-MACHO catalyst,[27b,40] ethylation of the N−H group results in a similar outcome to that of Noyori catalyst methylation;

DOI: 10.1021/jacs.6b11666
J. Am. Chem. Soc. 2017, 139, 1245−1260

however, the activation barrier for hydride transfer from the Ru complex to *anti*-methyl (*R*)-lactate is much less increased, by only 2.7 kcal·mol^{-1},[46] corresponding to a 97-fold decrease in the hydride transfer rate with respect to the corresponding N−H complex.[47] This nicely explains the observed 1.2% conversion of this substrate into the corresponding diol with the ethylated Ru-MACHO catalyst.[27b]

2.2. Identification of a Coordinatively Saturated (18e$^-$) M/NH Complex with a Wide H−N−M−X (X = Cl, H) Dihedral Angle and Synthesis of Its Methylated Analog. Is an N−H functionality *always* needed for ultimate turnover[48] and C═O/C═C chemoselectivity (and ultimately enantioselectivity[49]) of the catalytic reaction? Indeed, at the heart of this matter, we would like to argue that extremely high TEs as well as high C═O/C═C chemoselectivities are not only due to the presence of this functionality (which, according to our point of view,[18] provides a sufficiently stabilizing N−H···O HBI within rate-determining TSs, but does not serve to transfer a H$^+$) but also largely due to the fact that the C═O group reduction itself necessarily proceeds in the outer-sphere.[42b] This is in contrast to "slow" (and low C═O/C═C chemoselective) hydrogenation catalysts operating via the classical Schrock−Osborn pathway,[6] which necessarily proceeds via inner-sphere reduction of the C═O group.[7] The question posed in the beginning of the section could indeed be viewed as rhetorical for (pre)catalysts shown in Figure 1 and their reported substrates, and perhaps for some other (pre)catalysts, in particular ones in which the key structural parameter is planarity of the H−N−M−X dihedral angle (X = H, Cl, etc.), which is equivalent to the presence of an intramolecular M−H···H−N dihydrogen-bonding interaction within the actual catalyst.[50] However, we speculate that the answer to the question above can become relevant via consideration of a group of (pre)catalysts possessing sufficiently wide H−N−M−X dihedral angles, Figure 4.[51]

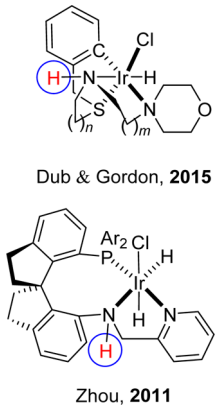

Figure 4. Ir/NH (pre)catalysts with wide H−N−Ir−Cl dihedral angles.

Indeed for such catalysts, assuming that a carbonyl substrate is reduced within the outer-sphere,[42b] due to geometrical factors, the corresponding N−H···O HBI could be absent within rate-determining **TS$_d$**- and/or **TS$_e$**-type transition states as shown in Figure 2b; i.e., the ligand would behave as *noncooperative*.[18] However, reaction could still proceed through the same reaction channel as shown in Scheme 4. From this perspective, alkylation of the N−H functionality may alter the electron density at the metal (and hydride) atom and/or arguably result in a potentially more stable catalyst. Indeed, 16e$^-$ amido complexes obtained by formal dehydrogenation/dechlorination of 18e$^-$ MX/NH (X = H, Cl) can be a very unstable species.[52] The issue of molecular catalyst stability is a very important factor for practical catalytic hydrogenations,[53] because all organometallic compounds are intrinsically unstable from an entropic point of view. It is thus evident that a "deprotonatable" N−H functionality could be potentially "the weakest link" in these hydrogenations, which are as a matter of fact typically carried out under basic conditions.

The N−H ligand **1** used in this work[54] was prepared by *N*-alkylation of commercial 3-morpholinopropylamine with 3-bromopropyl benzyl sulfide (BnSCH$_2$CH$_2$CH$_2$Br)[55] as shown in Scheme 6 following the synthetic procedure established for ENENES ligands.[51a,56]

The synthesis of *N*-methylated ligand **2** was accomplished by a formic acid−formaldehyde methylation (Eschweiler−Clarke reaction)[57] of **1**. Complexes **Ir1**[58] and **Ir2** were synthesized using the synthetic methodology recently discovered in the preparation of κ^4[*N*,*N*′,*S*,*C*]-tetradentate Ir complexes via the reaction of [IrCl(η^2-COE)$_2$]$_2$ (COE = cyclooctene) and 2 equiv of an ENENES ligand containing an −SBn auxiliary.[51a] The X-ray structures of **Ir1** and **Ir2** are shown in Figures 5 , 6, and 7.

In contrast to **Ir1**, complex **Ir2** crystallized as two independent molecules as shown in Figures 6 and 7, respectively. These molecules differ from each other in the conformation of the *N*-alkyl morpholine moiety, which adopts equatorial (Molecule ***a***) and axial (Molecule ***b***) conformations, respectively. We remind the reader that equatorial/axial conformations are separated by ∼1 kcal·mol^{-1} in a morpholine molecule itself.[59] In general, the X-ray structures of **Ir1** and **Ir2** are similar, but differ in the conformation of either the six-membered (IrNCCCN) iridacycle ring or morpholine auxiliary, the latter of which adopts an equatorial and/or axial conformation. We have observed such conformations in other related κ^4[*N*,*N*′,*S*,*C*]-tetradentate Ir complexes.[51a] The corresponding dihedral angle (Cl−Ir−N−CH$_3$) within complex **Ir2** increases by ∼10° relative to that parent (Cl−Ir−N−H) within **Ir1** upon methylation of the N−H functionality, presumably in order to minimize unwanted steric repulsion.

2.3. Catalytic Efficiencies of Ir1 and Its Methylated Analog Ir2 in the Hydrogenation of Carbonyl Functionalities. Scheme 7, Table 1, and Table S11 compare the catalytic efficiencies of both complexes in the hydrogenation of selected aromatic ketones.[54]

Both catalysts **Ir1** and **Ir2** quantitatively hydrogenate nonenolizable ketone **K1** after 0.5−3 h at 40 °C in methanol with a substrate-to-catalyst ratio (S/C) of 1000 to 50 000 (runs 1−4, Table S11). No transfer hydrogenation takes place under these conditions (runs 5−6, Table S11). Notably, in attempts to prepare the reaction mixture in a contaminated glovebox atmosphere (i.e., in the presence of some degree of oxygen), catalysis still occurs; however, methylated complex **Ir2** is almost two times more active than **Ir1** (runs 7−8, Table S11), suggesting its greater stability in the presence of oxygen. The reaction even works with higher S/C values, i.e., 250 000 (runs 1−2, Table 1) and 1 000 000 (runs 9−12, Table S11), whereupon **Ir2** exhibits slightly better activity. Methanol is the solvent of choice for the present reaction, since much slower catalysis occurs in aprotic THF and toluene with both catalysts (runs 13−16, Table S11).[60] Substrates **K2**, **K3**, and **K6** can also be qualitatively hydrogenated with both catalysts (runs

DOI: 10.1021/jacs.6b11666
J. Am. Chem. Soc. 2017, 139, 1245−1260

Scheme 6. General Synthetic Route to Complexes Ir1 and Ir2

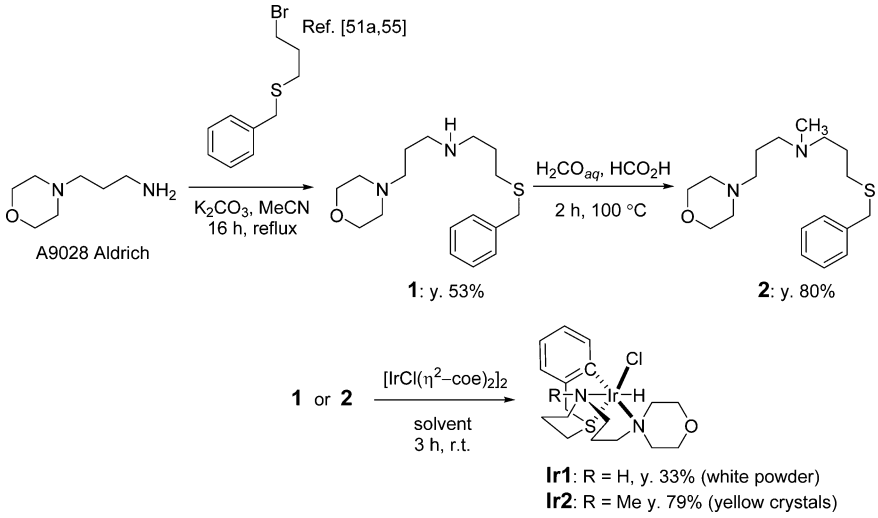

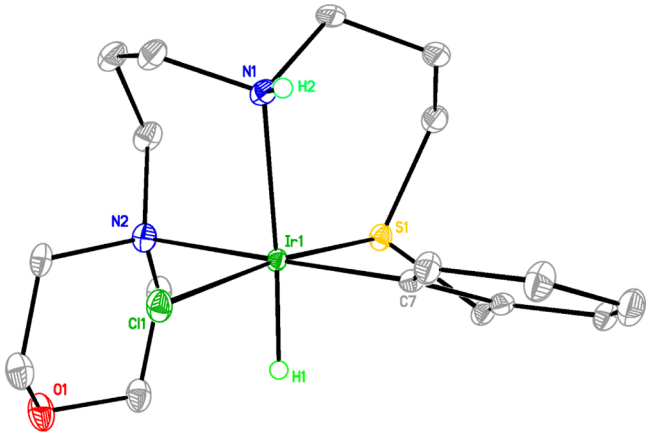

Figure 5. 50% thermal ellipsoids ORTEP plot for complex **Ir1**. Noncritical H atoms are omitted for clarity. Selected bond distances (Å): Ir1–H1 = 1.49 (7); Ir1–C7 = 2.027 (2); Ir1–N1 = 2.243 (2); Ir1–N2 = 2.307 (2); Ir1–S1 = 2.2435 (6); Ir1–Cl1 = 2.4050 (5). Selected dihedral angle (deg): Cl1–Ir1–N1–H2 = 52.4 (4).

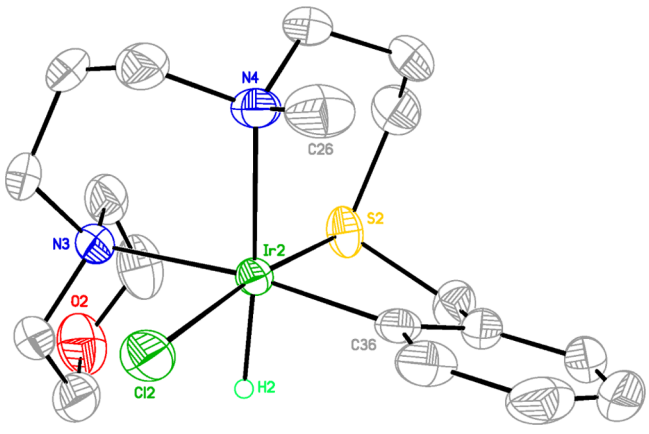

Figure 6. 50% thermal ellipsoids ORTEP plot for complex **Ir2** (Molecule ***a***). Noncritical H atoms are omitted for clarity. Selected bond distances (Å): Ir2–H2 = 1.52 (4); Ir2–C36 = 2.032 (3); Ir2–N3 = 2.375 (3); Ir2–N4 = 2.334 (2); Ir2–S2 = 2.2500(8); Ir2–Cl2 = 2.3835 (8). Selected dihedral angle (deg): Cl2–Ir2–N4–C26 = 62.42 (0.21).

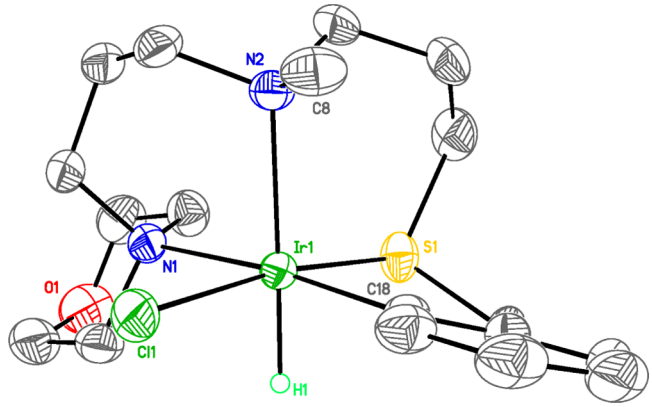

Figure 7. 50% thermal ellipsoids ORTEP plot for complex **Ir2** (Molecule ***b***). Selected bond distances (Å): Ir1–H1 = 1.45 (4); Ir1–C18 = 2.033 (3); Ir1–N1 = 2.328 (2); Ir1–N2 = 2.317 (2); Ir1–S1 = 2.2474 (8); Ir1–Cl1 = 2.3871 (8). Selected dihedral angle (deg): Cl1–Ir1–N2–C8 = 65.58 (0.20). The present view was obtained by the mirror inversion from original Molecule ***b***.

3–6, 11–12, Table 1), whereas almost no catalysis occurs for fluorinated **K4** and **K5**, possibly because of the formation of inactive species (runs 7–10, Table 1).[61]

Both **Ir1** and **Ir2** promote rapid and chemoselective hydrogenation of methyl styryl ketone **K7**, Scheme 8 (reaction 3). The substrate is hydrogenated with a C=O/C=C chemoselectivity of ∼94% by **Ir1** and ∼93% for **Ir2**, respectively.

The turnover number (TON)[5c] reaches >99 000 for **Ir1** and >81 000 for **Ir2**, after 5 h at 40 °C.[62,63] We remind the reader that high TEs and high C=O/C=C chemoselectivity were two arguments for Noyori to propose his nonclassical mechanism based on outer-sphere reduction of C=O group.[4] In contrast, the opposite is observed for catalysts that are believed to operate via a classical inner-sphere mechanism, Scheme 8 (reactions 4–5).[64]

Ir1 and **Ir2** were also used to hydrogenate methyl benzoate **E1** (less electrophilic reagent) in THF; however, decomposition took place at elevated temperatures as evidenced by the formation of a black precipitate (runs 31–32, Table S11). On the other hand, the reaction proceeded rapidly with

DOI: 10.1021/jacs.6b11666
J. Am. Chem. Soc. 2017, 139, 1245–1260

Scheme 7

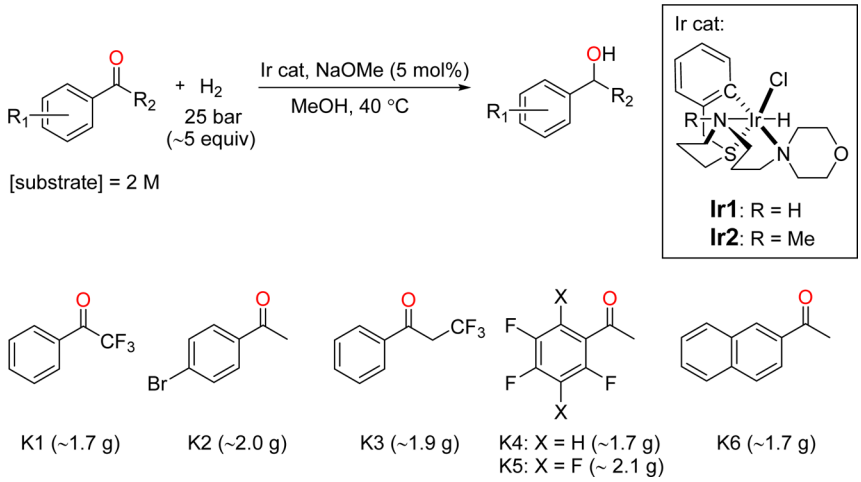

Table 1. Catalytic Hydrogenation of Carbonyl Substrates with Catalysts Ir1 and Ir2[a]

run	cat.	subs	S/C	time (h)	conv.[b] (%)[b]	yield[b] (%)[b]
1	Ir1	K1	250 000	3	>99	>99
2	Ir2	K1	250 000	3	>99	>99
3	Ir1	K2	1000	1	>99	>99
4	Ir2	K2	1000	1	>99	>99
5	Ir1	K3	1000	3	100	100
6	Ir2	K3	1000	3	100	100
7	Ir1	K4	50 000	3	~0	~0
8	Ir2	K4	50 000	3	~0	~0
9	Ir1	K5	1000	3	~0	~0
10	Ir2	K5	1000	3	~0	~0
11	Ir1	K6	1000	1	>98	>98
12	Ir2	K6	1000	1	>99	>99

[a]Standard reaction conditions: substrate (10 mmol), solvent (5 mL), 50 mL of Parr autoclave, argon atmosphere. [b]NMR (^{1}H or ^{19}F, rd = 10 s).

Scheme 8. Issue of Reaction Rate and C=O/C=C Chemoselectivity as Argument Towards Outer versus Inner-Sphere Reduction of α,β-Unsaturated Ketones/Aldehydes

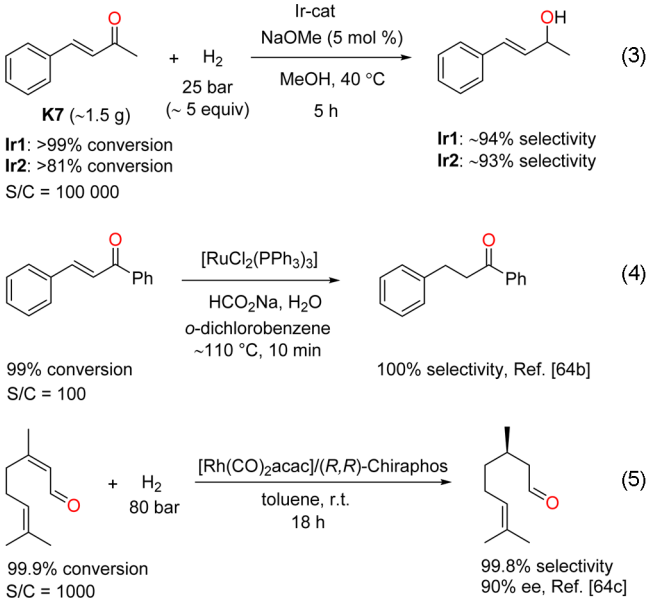

activated methyl trifluoroacetate ester **E2** in methanol, Scheme 9.

Scheme 9. Chemoselective Hydrogenation of Ester E2

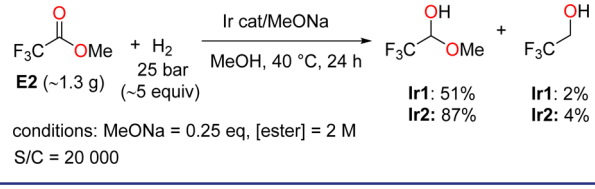

Interestingly, in contrast to ketones, a large excess of base, 25 mol % relative to substrate, is required for the practical conversion of **E2** into trifluoroacetaldehyde methyl hemiacetal by both catalysts with S/C = 20 000. Under these conditions, catalyst **Ir2** is almost twice as active as catalyst **Ir1**, providing a TON of ~19 000. Notably, almost no catalysis occurs if the base is present at 2.5 mol % under the same conditions. On the other hand if S/C is 2000, catalyst **Ir1** is almost 10 times more active than catalyst **Ir2**; see Table S12 for further details. These preliminary results could be suggestive, *among other possibilities*, of a twofold role of the large excess of base: (a) chemical modification of **Ir1** by MeONa[35a,65] and/or (b) electrophilic (Lewis) activation of the ester C=O group by "Na^+" as proposed in Scheme 10.

Note that activation of the C=O group is likely achieved via a type of a bifurcated noncovalent interaction between one sodium atom (ion) and two oxygen atoms in **E2** that may exist in the form of *anti-* and *syn-* conformers.[66] A large excess of

Scheme 10. Possible Activation of C(O)=O Group by MeONa (Na^+)

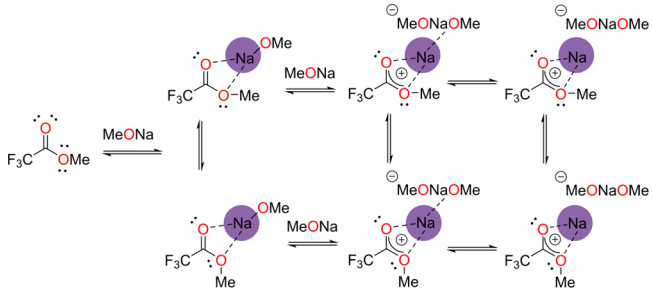

DOI: 10.1021/jacs.6b11666
J. Am. Chem. Soc. 2017, 139, 1245−1260

base could be required in order to keep this equilibrium toward the right. Obviously, ketones possessing a single oxygen atom cannot be activated in the same manner.

In fact, ^{19}F NMR experiments directly suggest the presence of equilibria between **E2** and MeONa, Figure S7a–c. The nature of these equilibria is not addressed in the present work, since a variety of species and their fast interconversions with respect the NMR time scale are possible, Scheme 10. Upon turnover (equivalent to the decrease of the ratio **E2**/MeONa), the group of resonances in the region of **E2** move toward the low field region of the spectrum. In contrast, the resonances corresponding to methyl trifluoroacetate and 2,2,2-trifluoroethanol are always sharp, suggesting that these compounds are not involved in any notable equilibria with MeONa.

2.4. Computational Study of the Mechanism of Catalytic Hydrogenation of Methyl Trifluoroacetate (E2) into the Corresponding Hemiacetal with Ir1 and Ir2. Chemoselective catalytic hydrogenation of **E2** into trifluoroacetaldehyde methyl hemiacetal, rather than 2,2,2-trifluoroethanol as shown in Scheme 9, represents an important chemical reaction, since the hemiacetal is one of the most important synthons in the production of various fluorinated chemicals containing CF_3-groups[67] that are used in medicinal chemistry,[68] agrochemical,[69] and materials research.[70] Previous studies with the Ru-MACHO catalyst demonstrated that accumulation of this product is possible under kinetic control, whereas the thermodynamic product is 2,2,2-trifluoroethanol.[37] Benchmark studies[51a] and studies presented in Scheme 9 confirm that (pre)catalyst **Ir2** is currently the most efficient catalyst capable of chemoselectively hydrogenating **E2** into the corresponding hemiacetal with reasonable ~18 000 turnovers.

In the present work, we report the computational analysis of the catalytic hydrogenation of methyl trifluoroacetate (**E2**) into the corresponding hemiacetal with **Ir1** and **Ir2** under high MeONa concentration. The analysis is performed on full catalyst models, with an extended basis set and by accounting for solvent effects via the introduction of nonspecific solvation; see Supporting Information (SI) for more details. A computational study for both (pre)catalysts was performed, assuming that the actual intermediate of each catalytic reaction is *cis*-IrH_2 dihydride complex $\mathbf{A^X}$ (X = H or Me), obtained in the beginning of the process from **Ir1** and **Ir2** under the conditions of the reaction, as is typically the case with other similar coordinatively saturated (18e$^-$) (pre)catalysts.[37,71] The computational analysis was initiated by a proper conformational search followed by determination of the influence of implicit versus implicit/explicit solvation to model thermodynamics of Na-amidato complexes and completed by probing the possibility of the reaction to follow the classical Schrock–Osborn (inner-sphere) mechanism. Full details are available in the SI. We note here that there is no need to include explicit solvent molecules[72] in order to model the thermodynamics of Na-amidato complexes; see Figure S10 for details.

2.4.1. Minimum Energy Hydride Transfer (MEHT) from cis-Ir Dihydride A^X (X = H, Na, Me) and E2. The Effect of N–H Group Methylation on the Relative Rate of Hydride Transfer. There are eight possibilities for outer-sphere hydride transfer from complex $\mathbf{A^H}$ to the carbon atom of the carbonyl group in **E2**. These originate from two inequivalent hydrides within the complex, two conformers of **E2** (*anti* and *syn*),[73] and two possibilities (*Re*- and *Si*-face) for substrate approach, Figure 8.

There are multiple transition states for each possible hydride transfer scenario originating from numerous possible geometrical combinations within the CSC along the Ir–H–C vector. Various constrained potential energy surface scans (CPESSs) were performed, and 24 of the most stable transition states for each possibility of $\mathbf{A^X}$–**E2** CSC are reported in SI, Figures S11–S12. The identified MEHT is independent of the nature of X, and for X = H, the corresponding computed intrinsic reaction coordinate (IRC)[74] is shown in Figure 9.

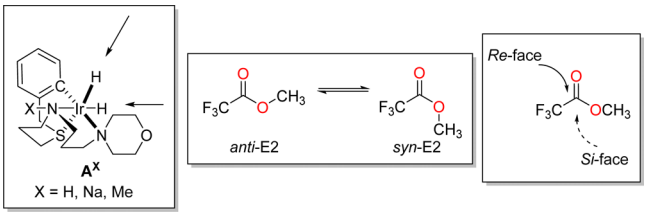

Figure 8. Definition of 8 possible transition states to transfer the hydride to **E2**. For all X, it gives a total of 24 transition states; see SI for details.

In agreement with an expected *trans*-effect (SR_2 > NHR_2), the MEHT from $\mathbf{A^H}$ to **E2** occurs selectively in the position *trans*- to the S atom. The substrate approaches the hydride atom within the *Re*-face position and in the form of the *anti*-**E2** conformer, in agreement with the unfavorable thermodynamics *anti*-**E2** → *syn*-**E2** ($\Delta G^\circ_{298\ K}$ = 7.45 kcal·mol^{-1}). However, in contrast to the Noyori and Ru-MACHO catalysts shown Figure 3, the N–H group within $\mathbf{A^H}$ is not involved in stabilization of the TS of type $\mathbf{TS_d}$[75] (this appears as $\mathbf{TS_1^H}$ in Figure 9) via any N–H···O HBI; i.e., the ligand is in fact *noncooperative*[18] for this reaction. Similarly, the N–H group neither activates the substrate in van der Waals (vdW) complex $\mathbf{1^H{\cdots}E2}$ (there is no N–H···O=C HBI) nor stabilizes the inner-sphere ion-pair complex $\mathbf{B^H}$ via the same interaction, Figure 9. Methylation of the N–H functionality neither changes the nature of the MEHT nor significantly affects the geometry of the TS corresponding to hydride transfer. This appears as $\mathbf{TS_1^{Me}}$ in Figure 9. The computed activation barrier for hydride transfer upon methylation increases by only 1.7 kcal·mol^{-1}, corresponding to a 17 times decrease in reaction rate with respect to the analogous N–H complex. This is significantly less than the corresponding values *computed* for the Noyori and Ru-MACHO catalysts, Figure 3.

In our previous attempts to model outer-sphere hydride transfer from the Noyori catalyst to acetophenone[35a] (or other similar catalysts[35b,37]), various CPESSs were also performed along the C(O)–H(Ru) coordinate (M = Ru). Numerous geometrical arrangements of vdW complexes are possible within the CSC between two limit structures ***a*** and ***b*** (preliminarily optimized for each scan) in Figure 10.

In all cases, the corresponding scans effectively converged to the same pre-TS complex in which the C=O group is always placed more or less in a parallel fashion with respect to the M–N vector and the substrate is stabilized by a N–H···O HBI. Therefore, one N–H moiety within the Noyori catalyst also orients the substrate, making possible only two minimum energy transition states, which are *Re*- and *Si*-face positioned, to extract the hydride atom. In contrast, we never found any similar pre-TS complex with N–H···O HBI in modeling the same transfer from complex $\mathbf{A^H}$ and **E2** within the MEHT. The reason for this is likely due to the unfavorable thermodynamics of ~5 kcal·mol^{-1}, required to rotate the dihedral angle H–N–Ir–H, initially ~60° in the most stable conformation, to the

DOI: 10.1021/jacs.6b11666
J. Am. Chem. Soc. 2017, 139, 1245–1260

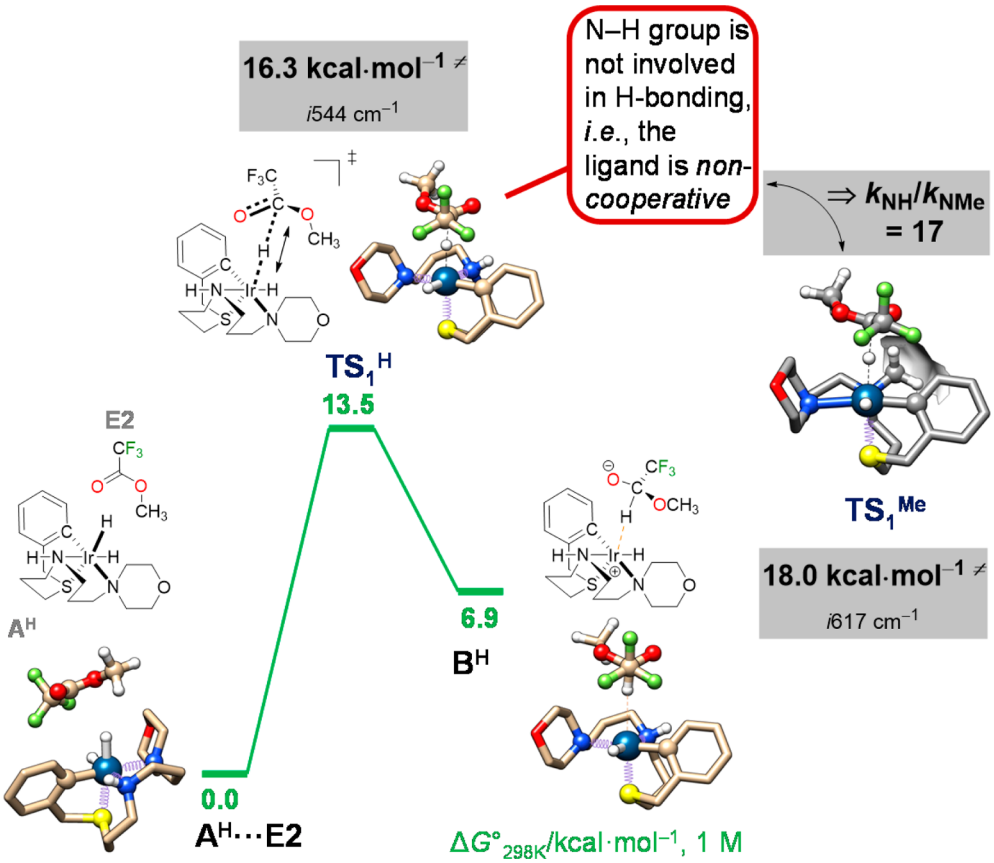

Figure 9. (Left) IRC path for the hydride transfer from the *cis*-Ir dihydride complex $\mathbf{A}^{\mathbf{H}}$ and **E2**, computed at DFT/ωB97X-D/ECP60MDF_VTZ(Ir)/6-311++G**(all others)/SMD(methanol) level of theory. ≠Activation barrier with respect to separate reagents. (Right) The computed effect of N–H group methylation on the relative rate of hydride transfer.[43]

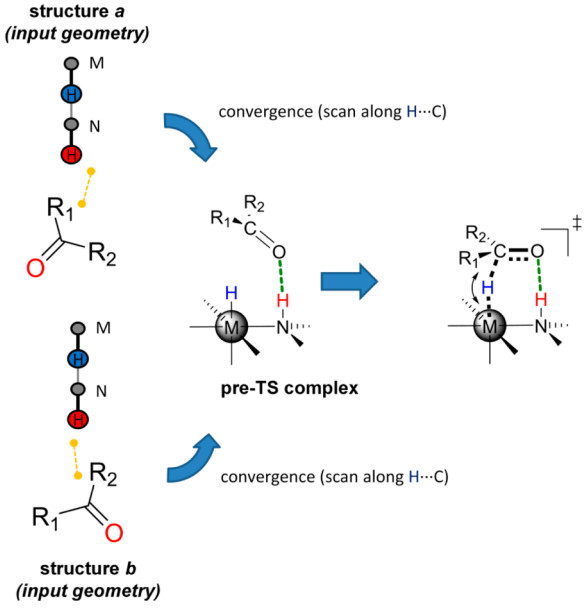

Figure 10. Computational modeling of the outer-sphere hydride transfer between the Noyori catalyst (or other similar catalysts[35b,37]) and acetophenone performed in previous work.[35a]

conformation in which the angle is closer to planarity, i.e. ∼16° as with Noyori's catalyst; see Figure S9.

2.4.2. Catalytic Cycle. Identity and Energetics of H⁻/H⁺ OSHM. The computed reaction path corresponding to the concept of H⁻/H⁺ OSHM for the hydrogenation of **E2** into the corresponding hemiacetal with the active forms of **Ir1** and **It2** under high MeONa concentration is shown in Scheme 11. Because, experimentally, the reaction is carried out in the presence of 25 mol % MeONa, crossover with catalytic cycle II shown in Scheme 4 was not considered.

After selective outer-sphere hydride transfer via $\mathbf{TS}_1^{\mathbf{X}}$ from the *cis*-Ir dihydride complex $\mathbf{A}^{\mathbf{X}}$ to **E2**, the inner-sphere ion-pair $\mathbf{B}^{\mathbf{X}}$ stabilized by an C–H···M interaction is obtained, Scheme 11. Dissociation of this ion pair and further H_2 coordination affords the η^2-H_2 ion-pair complex $\mathbf{C}^{\mathbf{X}}$, stabilized by an Ir–$(\eta^2$-$H_2)^+$···OCH(CF_3) (OMe) HBI.[76] Deprotonation of the η^2-H_2 ligand by the anion through $\mathbf{TS}_2^{\mathbf{X}}$ yields the catalyst-product dihydrogen-bonded complex $\mathbf{D}^{\mathbf{X}}$, completing the catalytic cycle, $\Delta G_r^{\circ}{}_{298\ \mathrm{K}} = -5.3$ kcal·mol^{-1}. Similarly to $\mathbf{TS}_1^{\mathbf{X}}$, there is no N–H···O HBI in $\mathbf{TS}_2^{\mathbf{X}}$ (X = H, Me).

Both **Ir1** and **Ir2** share the same TDTSs and turnover-determining intermediates (TDIs),[38] which are $\mathbf{TS}_1^{\mathbf{X}}$ and $\mathbf{A}^{\mathbf{X}}$ (X = H or Me), respectively. The computed energetic span[38] for the Ir/NH catalyst $\mathbf{A}^{\mathbf{H}}$ is 16.3 kcal·mol^{-1}. This gives a turnover frequency (TOF) of 7 s^{-1} under standard conditions, which compares well with the experimental value of 5 s^{-1} at 40 °C.[51a] However, in the presence of a large excess of MeONa, NH/NNa exchange may potentially occur as is likely the case with the Noyori catalyst.[35a,65,77] According to computational analysis, this exchange indeed takes place in the reaction pool of $\mathbf{A}^{\mathbf{H}}$; however, the NH/NNa substitution does not affect the nature of the TDTS and TDI (still $\mathbf{A}^{\mathbf{H}}$ and $\mathbf{TS}_1^{\mathbf{H}}$), and correspondingly the computed energetic span.[78] This does not

DOI: 10.1021/jacs.6b11666
J. Am. Chem. Soc. 2017, 139, 1245–1260

Scheme 11. Reaction Path Corresponding to the Concept of H^-/H^+ OSHM for the Hydrogenation of E2 into Its Hemiacetal with Active Forms of Ir1 and Ir2 under Basic Conditions Computed at the DFT/ωB97X-D/ECP60MDF_VTZ(Ir)/6-311++G(All Others)/SMD(Methanol) Level of Theory[a]**

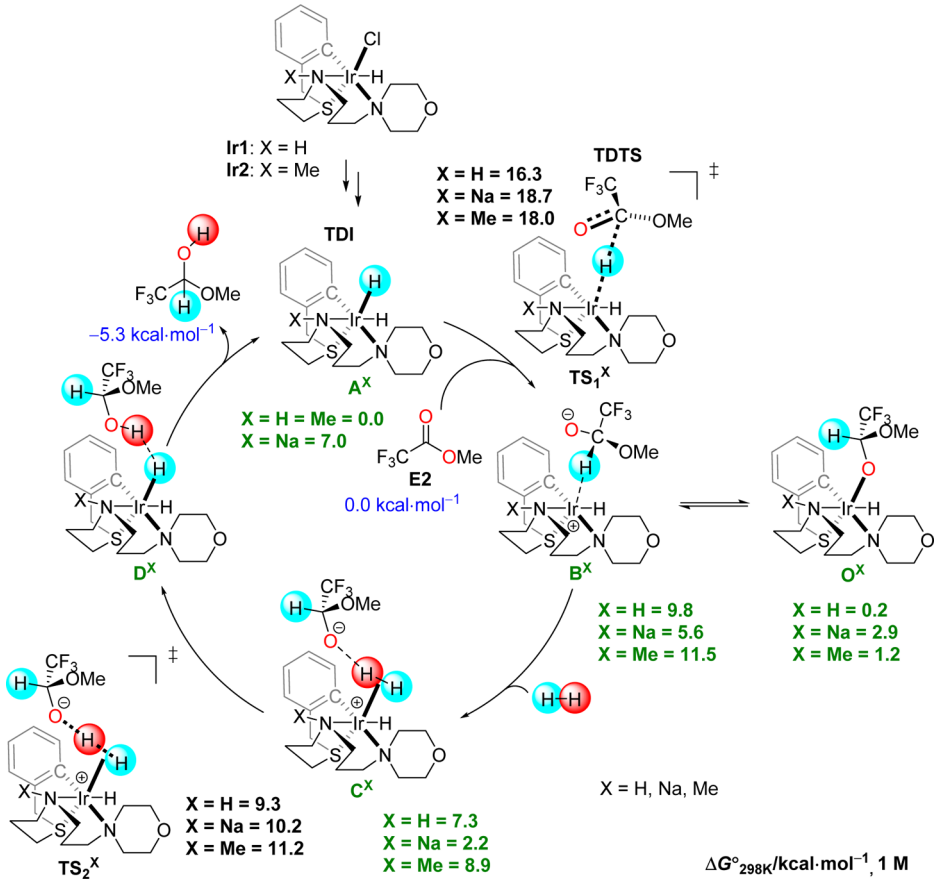

[a]The energy of sodium amidato complexes is computed from the reaction $\mathbf{A^H}$ + MeONa = $\mathbf{A^{Na}}$ + MeOH. For $\mathbf{A^H}/\mathbf{A^{Na}}$ all the energies are calibrated against $\mathbf{A^H}$. For $\mathbf{A^{Me}}$, all the energies are calibrated against $\mathbf{A^{Me}}$. The thermodynamics of the reaction **E2** + H_2 is shown in blue.

explain why a large excess of base is needed for the TOF. Therefore, either the quantitative agreement between computed and experimental TOFs is fortuitous or the base plays a different role in the reaction. For example, the base may electrophilically activate the ester via the equilibria proposed in Scheme 10. More benchmark studies are needed to support/disprove these assumptions. A detailed investigation of the overall effect of the base is no doubt warranted in the future, but is not the purpose of the present work.

The computed energetic span of 18.0 kcal·mol^{-1} (TOF = 0.4 s^{-1} under standard conditions) for catalyst $\mathbf{A^{Me}}$ is 1.7 kcal·mol^{-1} uphill from the same in $\mathbf{A^H}$ on a free energy scale, suggesting, that outer-sphere hydride transfer with **Ir2** (and the extrapolated catalytic reaction rate with **Ir2**) should be ∼20 times slower than with **Ir1**, assuming no decomposition occurs. One must admit, however, that this energy difference undoubtedly lies within the accuracy of the DFT computations (plus possible errors from conformational analysis, since not all conformers are considered) and, therefore, is rather a testament to isoenergetic or very close catalytic reaction activation barriers for **Ir1** and **Ir2**. Alternatively, the slightly better experimentally observed activity with **Ir2** for selected substrates could be due to the fact that catalyst **Ir2** is simply more stable than **Ir1**. This hypothesis is actually supported by runs 7−8, Table S11. Regardless of actuality, the computations herein support our assessment that there could be M/NH catalysts in which a N−H···O HBI could be fully absent within $\mathbf{TS_d}/\mathbf{TS_e}$ type transition states. Also the same computations support that the catalytic reaction for an M/NH and its alkylated version could proceed via the same reaction channel, with comparable and relatively small activation barriers (energetic spans) for the catalytic reaction of ∼17.0 kcal·mol^{-1}. The possibility that reaction proceeds via the classical Schrock−Osborn (inner-sphere) mechanism was excluded based on experimental observations (high TEs and high C═O/C═C chemoselectivities) and theoretical analysis; see SI for more details.

2.5. Strength of the N−H···O HBI and the Size of a Substrate. The Effect of N−H Group Methylation on the Relative Rate of Hydride Transfer from the Ru-MACHO Catalyst to CO_2. During the preparation of this manuscript,[79] Ding described a hydrogenative transformation of CO_2 and morpholine into 4-formylmorpholine catalyzed by Takasago's Ru-MACHO catalyst,[80] Scheme 12.

Although the reaction is not a net hydrogenation of CO_2 into HCO_2H (or HCO_2^-),[81] methylation of the N−H functionality does not inhibit catalytic activity, but instead results in a catalyst demonstrating comparable efficiencies. The methylated catalyst is extremely efficient (practical) and ultimately displays >2 × 10^6 turnovers, Scheme 12. The results described by Ding suggest that not only a relatively wide H−N−M−X dihedral angle (and correspondingly the absence of an intramolecular M−X···H−N interaction) within an M/NH catalyst but also

DOI: 10.1021/jacs.6b11666
J. Am. Chem. Soc. 2017, 139, 1245−1260

Scheme 12. Catalytic Reaction Described by Ding[80]

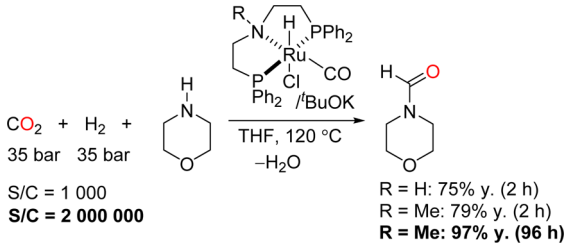

the nature of the substrate itself could be important with respect to providing the answer in the question raised in the title of the paper, even if an M/NH catalyst has a narrow H–N–M–X dihedral angle as Ru-MACHO does. From this perspective, carbon dioxide (CO_2) is a unique molecule that is both relatively nonbulky (1D molecule) and possesses electron-deficient oxygen atoms (potentially forming a relatively weaker N–H···O HBI within $\mathbf{TS_d}$/$\mathbf{TS_e}$). The optimized geometries for the transition states corresponding to outer-sphere hydride transfer to CO_2 from the Ru-MACHO complex and its methylated analog and the structural parameters (D, d, θ),[82] shown in Figure 11, further confirm our assessment.

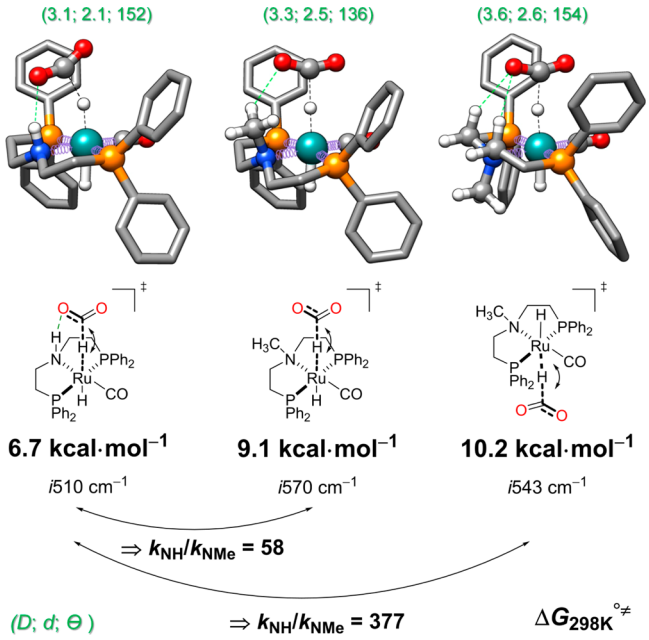

Figure 11. Computed effect of N–H group methylation on the relative rate of hydride transfer from the Ru-MACHO complex to CO_2.[43] TSs optimized at the DFT/ωB97X-D/ECP28MDF_VTZ-(Ru)/6-311++G**(all others)/SMD(THF) level of theory (for stick representations, selected H atoms are omitted for clarity).

In contrast to *anti*-methyl (*R*)-lactate as shown in Figure 3, CO_2 forms a much weaker N–H···O HBI within the TS of type $\mathbf{TS_d}$.[82] Methylation of the N–H functionality almost does not change the relative position of CO_2 during the outer-sphere extraction of the hydride atom in this case; furthermore, the corresponding TS is stabilized by a relatively weak C–H···O HBI.[82c,83] Although such an interaction was also noticed in the CSC between ethylated Ru-MACHO and *anti*-methyl (*R*)-lactate as shown in Figure 3, there is apparently much less repulsion within the CSC due to the 1D nature of CO_2. As a result, the activation barrier of hydride transfer to CO_2 upon methylation increases by only 2.4 kcal·mol^{-1}. This corresponds to a *computed* decrease in the hydride transfer rate of only 58 times with respect to the analogous N–H complex!

3. CONCLUSIONS

Traditionally, the origin of high rates and chemoselectivities in the reduction of carbonyl functionalities with M/NH bifunctional Noyori-type catalysts was associated with the conventional Noyori mechanism[22] in which the step of C=O reduction proceeds in the outer-sphere with the direct involvement of the ligand in the process through a concerted N–H proton transfer via $\mathbf{TS_a}$ in Figure 1. The 16e$^-$ amido complex generated by this transformation(s) serves as a "Lewis pair" to further regenerate the catalyst via cleavage of H_2 through $\mathbf{TS_b}$–$\mathbf{TS_c}$ in Figure 1. In a more recent interpretation, the N–H bond is not cleaved, but instead serves to stabilize the TDTSs $\mathbf{TS_d}$/$\mathbf{TS_e}$ via strong N–H···O HBIs, Figure 1.[18]

In this contribution, we show that the lack of N–H bond cleavage is consistent with the experimental observations that alkylation of N–H functionalities within M/NH bifunctional Noyori-type catalysts can still lead to catalytic activity, Figure 1. For the cases described in Figure 1, however, the resulting activity is detrimental to the reaction. A possible reason for this is explained in Figure 12: alkylation removes favorable H-bonding stabilization and increases the bulkiness around the hydride atom in the corresponding analog of $\mathbf{TS_d}$.

As a result, the relative rate of hydride transfer within the outer-sphere increases to an extent which depends on the

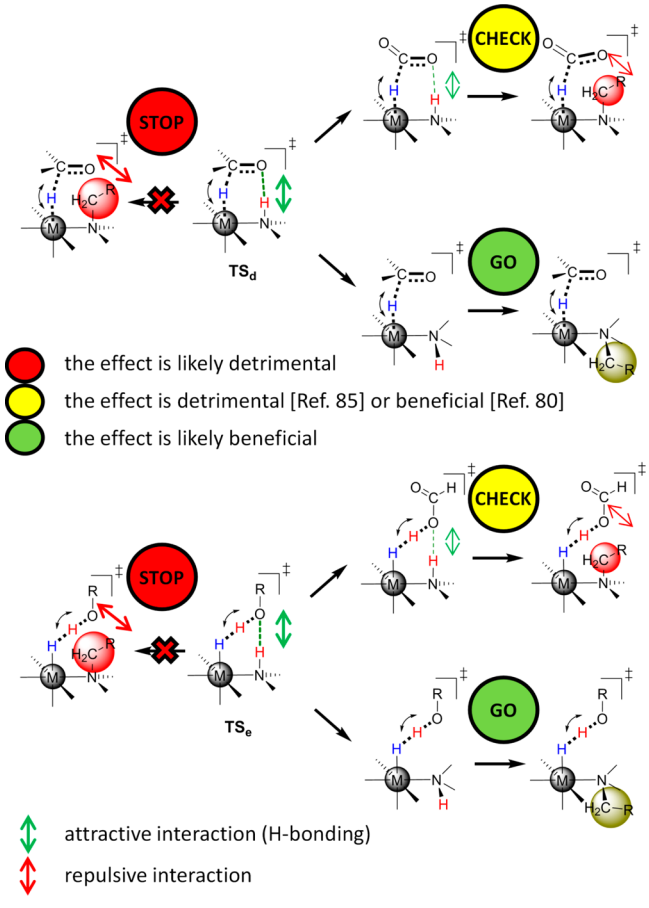

Figure 12. Diagram illustrating the effect of alkylation of N–H functionality in M/NH bifunctional Noyori-type catalysts.

DOI: 10.1021/jacs.6b11666
J. Am. Chem. Soc. 2017, 139, 1245–1260

nature of both the catalyst and substrate used. This fact agrees well with the experimental observations in Figure 1 and theoretical results in Figure 3. The same thinking is valid for TS_e, which in the catalytic cycles of hydrogenations always follows TS_d (but precedes it in the catalytic cycles of microscopically[20] reverse dehydrogenations). Therefore, the reason why alkylation of the N−H functionality within cases reported in Figure 1 is detrimental to catalytic reaction is a purely kinetic phenomenon.

We further show, based on two examples, that the complete absence of HBIs within TS_d/TS_e or decreasing its strength simultaneously with a decrease in substrate bulkiness is a condition under which alkylation of the N−H functionality within M/NH bifunctional Noyori-type catalysts may lead to improved activities in the reduction of carbonyl functionalities, Figure 12. In the case of Ir/NH catalyst **Ir1**, methylation of the N−H functionality does not inhibit catalytic activity, Table 1. Moreover the methylated complex **Ir2** affords similar or even better activities for selected substrates, Table S11. Computational analysis suggests that the origin of this unprecedented observation is the absence of any N−H···O HBI in the corresponding transition state during the outer-sphere hydride transfer, an identified TDTS in this reaction. This catalyst belongs to a presently very small group of catalysts possessing wide H−N−Ir−X dihedral angles (>50°, X = Cl, H).[51] In the case of the Ru/NH MACHO catalyst, which possesses a small H−N−Ru−H dihedral angle (∼0°), alkylation of the N−H functionality inhibits catalytic hydrogenation of methyl (*R*)-lactate,[27b] but favors the catalytic hydrogenation of CO_2.[80] Computational analysis suggests that the origin of this is simultaneously due to the initially weak N−H···O HBI in TS_d in Ru-MACHO, as well as the absence of any significant steric inhibition in the case of CO_2 (1D molecule) within the alkylated analog of TS_d in methylated Ru-MACHO.[84,85]

One may argue that the observed "efficiency" with the alkylated catalysts may additionally originate from the important, computationally intractable factor that is catalyst stability. In fact, all the computations indeed systematically predict slightly higher activation barriers for hydride transfer for methylated analogs of **Ir1**/**E2** and Ru-MACHO/CO_2.[86] Moreover, according to runs 7−8 in Table S11, catalyst **Ir2** is indeed more stable than **Ir1**. Similarly, the reaction temperature of 120 °C described for CO_2 hydrogenative transformation with the Ru/NH Ru-MACHO is relatively high for a molecular catalyst and thermal decomposition may potentially occur, enabling "more efficient" catalysis with the Ru/NMe analog. Whatever the case, methylation of the N−H functionality within these two Ir/NH and Ru/NH (pre)catalysts leads to improved activities and practical catalysts, which reach turnover numbers of ∼80 000 for (pre)catalyst Ir/NMe **Ir2** (substrate **K7**, 5 h, 40 °C, ∼ 93% C═O/C═C chemoselectivity) and ∼2 000 000 for the (pre)catalyst Ru/NMe Ru-MACHO (substrate CO_2, 96 h, 120 °C).

In conclusion, the revised mechanism of the Noyori hydrogenation reaction[35a] effectively explains the origin and extent of detrimental catalytic activity for M/NH bifunctional Noyori-type catalysts in which a hydrogen atom within a N−H functionality was replaced with an alkyl group. This and parallel[80] work represent the first described examples in which alkylation of the N−H functionality *can lead to improved catalytic activities* in the reduction of a variety of carbonyl functionalities. The reasons for these "unexpected" activities have been summarized above. Researchers can now explore more catalyst−substrate combinations in the laboratory through a trial-and-error approach, with the realization that that an N−H functionality does not necessarily have to participate in the reaction via its bond cleavage/formation only because the reaction mechanism is "plausible", is "accepted", or "can simply be computed through location of intermediates and transition states".[87]

■ ASSOCIATED CONTENT

Supporting Information

The Supporting Information is available free of charge on the ACS Publications website at DOI: 10.1021/jacs.6b11666.

Experimental and computational details, hydrogenation of **E2** under different S/C and base concentrations, ^{19}F NMR spectra of **E2**/MeONa, conformational analyses, implicit versus implicit/explicit solvation to model thermodynamics of Na-amidato complexes, computational probing the reaction pathway through a classical Schrock−Osborn (inner-sphere) mechanism, tables of energy data and Cartesian coordinates for optimized geometries and other details (PDF)

Crystallographic data (CIF, CIF)

■ AUTHOR INFORMATION

Corresponding Authors

*pdub@lanl.gov

*jgordon@lanl.gov

ORCID

Pavel A. Dub: 0000-0001-9750-6603

Notes

The authors declare no competing financial interest.

■ ACKNOWLEDGMENTS

This work was supported via the award of a J. Robert Oppenheimer (JRO) Distinguished Postdoctoral Fellowship to P.A.D. at LANL. Some computations in this work were performed at the Center for Integrated Nanotechnologies, an Office of Science User Facility operated for the U.S. Department of Energy (DOE) Office of Science by Los Alamos National Laboratory (Contract DE-AC52-06NA25396) and Sandia National Laboratories (Contract DE-AC04-94AL85000). Others were performed by using Darwin Computational Cluster at Los Alamos National Laboratory. Crystallographic data for **Ir1** and **Ir2** are available free of charge from the Cambridge Crystallographic Data Centre under reference numbers 1490846−1490847.

■ REFERENCES

(1) Kubas, G. J. *Chem. Rev.* **2007**, *107*, 4152.

(2) (a) Ayad, T.; Phansavath, P.; Ratovelomanana-Vidal, V. *Chem. Rec.* **2016**, *16*, 2750. (b) Blaser, H.-U.; Pugin, B.; Spindler, F. *Top. Organomet. Chem.* **2012**, *42*, 65. (c) Imamoto, T. In *Hydrogenation*; Karamé, I., Ed.; InTech: 2012. (d) de Vries, J. G., Elsevier, C. J., Eds. *Handbook of Homogeneous Hydrogenation (3 Vols.)*; Wiley-VCH Verlag GmbH & Co. KGaA: 2007.

(3) Magano, J.; Dunetz, J. R. *Org. Process Res. Dev.* **2012**, *16*, 1156.

(4) Noyori, R.; Ohkuma, T. *Angew. Chem., Int. Ed.* **2001**, *40*, 40.

(5) (a) Kozuch, S. *ACS Catal.* **2013**, *3*, 380. (b) Lente, G. *ACS Catal.* **2013**, *3*, 381. (c) Kozuch, S.; Martin, J. M. L. *ACS Catal.* **2012**, *2*, 2787. (d) Herrmann, W. A.; Cornils, B. *Angew. Chem., Int. Ed. Engl.* **1997**, *36*, 1048.

(6) Schrock, R. R.; Osborn, J. A. *J. Chem. Soc. D* **1970**, 567.

DOI: 10.1021/jacs.6b11666
J. Am. Chem. Soc. 2017, 139, 1245−1260

(7) (a) Malacea, R.; Poli, R.; Manoury, E. *Coord. Chem. Rev.* **2010**, *254*, 729. (b) Samec, J. S. M.; Bäckvall, J.-E.; Andersson, P. G.; Brandt, P. *Chem. Soc. Rev.* **2006**, *35*, 237. (c) Clapham, S. E.; Hadzovic, A.; Morris, R. H. *Coord. Chem. Rev.* **2004**, *248*, 2201.

(8) The notion of "inner-sphere" implies that a ketonic substrate *O*-coordinates to the metal within the catalytic cycle, and this coordination results in C═O bond polarization (activation) towards nucleophilic attack by hydride. However, when substrates containing two functional groups such as α,β-unsaturated ketones are used, the C═C group can also coordinate (π-coordination), and due to the competition of C═C and C═O bonds for the position *cis* to the hydride ligand, low C═O/C═C to high C═C/C═O chemoselectivities are obtained.

(9) Dahlenburg, L.; Götz, R. *Eur. J. Inorg. Chem.* **2004**, *2004*, 888.

(10) See, for example: Rahaman, S. M. W.; Daran, J.-C.; Manoury, E.; Poli, R. *J. Organomet. Chem.* **2016**, DOI: 10.1016/j.jorganchem.2016.10.009.

(11) Ohkuma, T.; Ooka, H.; Hashiguchi, S.; Ikariya, T.; Noyori, R. *J. Am. Chem. Soc.* **1995**, *117*, 2675.

(12) (a) Noyori, R.; Sandoval, C. A.; Muñiz, K.; Ohkuma, T. *Philos. Trans. R. Soc., A* **2005**, *363*, 901. (b) Noyori, R.; Kitamura, M.; Ohkuma, T. *Proc. Natl. Acad. Sci. U. S. A.* **2004**, *101*, 5356.

(13) The notion of "outer-sphere" implies that the reduction of a ketonic substrate proceeds without its preliminary coordination to a metal center. Because the C═O bond is initially polar, this explains the high level of C═O vs C═C chemoselectivity.

(14) (a) Zweifel, T.; Naubron, J.-V.; Büttner, T.; Ott, T.; Grützmacher, H. *Angew. Chem., Int. Ed.* **2008**, *47*, 3245. (b) Bi, S.; Xie, Q.; Zhao, X.; Zhao, Y.; Kong, X. *J. Organomet. Chem.* **2008**, *693*, 633.

(15) Hedberg, C.; Kaellstroem, K.; Arvidsson, P. I.; Brandt, P.; Andersson, P. G. *J. Am. Chem. Soc.* **2005**, *127*, 15083.

(16) (a) Ikariya, T.; Shibasaki, M. *Topics in Organometallic Chemistry: Bifunctional Molecular Catalysis*; Springer: New York, 2011; *Vol. 37*. (b) Ikariya, T. *Bull. Chem. Soc. Jpn.* **2011**, *84*, 1.

(17) Zhao, B.; Han, Z.; Ding, K. *Angew. Chem., Int. Ed.* **2013**, *52*, 4744.

(18) Dub, P. A.; Gordon, J. C. *Dalton Trans.* **2016**, *45*, 6756.

(19) Dub, P. A.; Ikariya, T. *ACS Catal.* **2012**, *2*, 1718.

(20) (a) Chandrasekhar, S. *Res. Chem. Intermed.* **1992**, *17*, 173. (b) Krupka, R. M.; Kaplan, H.; Laidler, K. J. *Trans. Faraday Soc.* **1966**, *62*, 2754. (c) Burwell, R. L.; Pearson, R. G. *J. Phys. Chem.* **1966**, *70*, 300.

(21) (a) Werkmeister, S.; Neumann, J.; Junge, K.; Beller, M. *Chem. - Eur. J.* **2015**, *21*, 12226. (b) Trincado, M.; Banerjee, D.; Grützmacher, H. *Energy Environ. Sci.* **2014**, *7*, 2464. (c) Friedrich, A.; Schneider, S. *ChemCatChem* **2009**, *1*, 72.

(22) We suggest that the term "conventional Noyori mechanism" be used to indicate the direct participation of the ligand in bond cleavage/formation events, regardless of the issue of concertedness for $\mathbf{TS}_a$ and $\mathbf{TS}_c$ in Scheme 3, i.e. whether or not these transition states are indeed concerted as depicted or actually stepwise; see text for further details and discussion.

(23) (a) Morris, R. H. *Chem. Rec.* **2016**, *16*, 2640. (b) Ohkuma, T.; Arai, N. *Chem. Rec.* **2016**, *16*, 2797. (c) Morris, R. H. *Acc. Chem. Res.* **2015**, *48*, 1494. (d) Khusnutdinova, J. R.; Milstein, D. *Angew. Chem., Int. Ed.* **2015**, *54*, 12236.

(24) One must note here that there were only two catalysts, the mechanisms of which were studied by the combination of all four methods (e.g., Noyori, Morris); the vast majority of M/NH bifunctional Noyori-type catalysts were studied exclusively computationally, primarily in the gas-phase and/or using simplified computational models. In the vast majority of these cases, the "study of the catalytic reaction mechanism" was limited to simple computations of the Noyori catalytic cycle (e.g. Scheme 3), rather than to actually study all pathways possible in this reaction; see ref 18.

(25) (a) Ito, M.; Hirakawa, M.; Murata, K.; Ikariya, T. *Organometallics* **2001**, *20*, 379. (b) Xie, J.-B.; Xie, J.-H.; Liu, X.-Y.; Zhang, Q.-Q.; Zhou, Q.-L. *Chem. - Asian J.* **2011**, *6*, 899.

(26) Ito, M.; Hirakawa, M.; Osaku, A.; Ikariya, T. *Organometallics* **2003**, *22*, 4190.

(27) (a) Saudan, L. A.; Saudan, C. M.; Debieux, C.; Wyss, P. *Angew. Chem., Int. Ed.* **2007**, *46*, 7473. (b) Kuriyama, W.; Matsumoto, T.; Ino, Y.; Ogata, O. Patent WO2011048727A1; Takasago Int. Co., 2011. (c) Ito, M.; Ootsuka, T.; Watari, R.; Shiibashi, A.; Himizu, A.; Ikariya, T. *J. Am. Chem. Soc.* **2011**, *133*, 4240. (d) Spasyuk, D.; Smith, S.; Gusev, D. G. *Angew. Chem., Int. Ed.* **2013**, *52*, 2538. (e) Filonenko, G. A.; Aguila, M. J. B.; Schulpen, E. N.; van Putten, R.; Wiecko, J.; Müller, C.; Lefort, L.; Hensen, E. J. M.; Pidko, E. A. *J. Am. Chem. Soc.* **2015**, *137*, 7620.

(28) Han, Z.; Rong, L.; Wu, J.; Zhang, L.; Wang, Z.; Ding, K. *Angew. Chem., Int. Ed.* **2012**, *51*, 13041.

(29) Bornschein, C.; Werkmeister, S.; Wendt, B.; Jiao, H.; Alberico, E.; Baumann, W.; Junge, H.; Junge, K.; Beller, M. *Nat. Commun.* **2014**, *5*, 4111.

(30) (a) Fujii, A.; Hashiguchi, S.; Uematsu, N.; Ikariya, T.; Noyori, R. *J. Am. Chem. Soc.* **1996**, *118*, 2521. (b) Morris, D. M.; McGeagh, M.; De Peña, D.; Merola, J. S. *Polyhedron* **2014**, *84*, 120. (c) Soni, R.; Cheung, F. K.; Clarkson, G. C.; Martins, J. E. D.; Graham, M. A.; Wills, M. *Org. Biomol. Chem.* **2011**, *9*, 3290.

(31) Ito, M.; Osaku, A.; Shiibashi, A.; Ikariya, T. *Org. Lett.* **2007**, *9*, 1821.

(32) (a) Arita, S.; Koike, T.; Kayaki, Y.; Ikariya, T. *Angew. Chem., Int. Ed.* **2008**, *47*, 2447. (b) Arita, S.; Koike, T.; Kayaki, Y.; Ikariya, T. *Chem. - Asian J.* **2008**, *3*, 1479.

(33) Matsunami, A.; Kayaki, Y.; Ikariya, T. *Chem. - Eur. J.* **2015**, *21*, 13513.

(34) The exception is the Zhou Ir (pre)catalyst, which is coordinatively unsaturated. The reason this catalyst is reported in Figure 1 is because Zhou classified it as an M/NH bifunctional Noyori-type catalyst, ref 25b. However, providing this catalyst is structurally and electronically similar to the Dahlenburg (pre)catalyst shown in Scheme 2, it may be possible that the former actually operates via the same inner-sphere mechanism. In fact, the effect of methylation of one or two NH functionalities in this catalyst is similar to the one observed with the Dahlenburg catalyst. Methylation does not surpress the catalytic reaction, but only results in a decrease in the reaction rate.

(35) (a) Dub, P. A.; Henson, N. J.; Martin, R. L.; Gordon, J. C. *J. Am. Chem. Soc.* **2014**, *136*, 3505. (b) Dub, P. A.; Ikariya, T. *J. Am. Chem. Soc.* **2013**, *135*, 2604.

(36) (a) Pavlova, A.; Meijer, E. J. *ChemPhysChem* **2012**, *13*, 3492. (b) Handgraaf, J.-W.; Meijer, E. J. *J. Am. Chem. Soc.* **2007**, *129*, 3099.

(37) Otsuka, T.; Ishii, A.; Dub, P. A.; Ikariya, T. *J. Am. Chem. Soc.* **2013**, *135*, 9600.

(38) Kozuch, S.; Shaik, S. *Acc. Chem. Res.* **2011**, *44*, 101.

(39) Dub, P. A. et al. Manuscript in preparation.

(40) Kuriyama, W.; Matsumoto, T.; Ogata, O.; Ino, Y.; Aoki, K.; Tanaka, S.; Ishida, K.; Kobayashi, T.; Sayo, N.; Saito, T. *Org. Process Res. Dev.* **2012**, *16*, 166.

(41) Wu, X.; Xiao, J. *Chem. Commun.* **2007**, 2449.

(42) (a) Comas-Vives, A.; Ujaque, G.; Lledós, A. In *Advances in Inorganic Chemistry*; Rudi van, E., Jeremy, H., Eds.; Academic Press: 2010; Vol. *62*, p 231. (b) Eisenstein, O.; Crabtree, R. H. *New J. Chem.* **2013**, *37*, 21.

(43) The ratio of the reaction rates of hydride transfer = k_{NH}/k_{NAlk} is calculated using absolute rate theory $\ln(k_{NH}/k_{NAlk}) = \Delta\Delta G_{298K}^{\circ}/RT$, where $\Delta\Delta G_{298K}^{\circ}$ is the standard Gibbs free energy difference in the activation barriers with respect to separate reagents.

(44) To minimize the effect of repulsion, the substrate now seeks stabilization (via the oxygen atom) with one C−H proton of the catalyst's phenyl group through an apparently weaker C−H···O HBI. As a result, during the outer-sphere hydride transfer, the relative position of acetophenone is displaced with respect to the initial geometry of the TS of Noyori's catalyst, Figure 3.

(45) In many catalytic cycles (because there are reactions that do not follow transition state theory and other assumptions do not work), the efficiency of the cycle is not determined solely by one transition state,

DOI: 10.1021/jacs.6b11666
J. Am. Chem. Soc. 2017, 139, 1245−1260

but rather from the energetic span defined from the turnover-determining transition state (TDTS), the turnover-determining intermediate (TDI), and sometimes the reaction driving force, ref 38. In catalytic cycles of hydrogenation with Noyori's and Ru-MACHO catalysts, hydride transfer is found as the TDTS, refs 35a, 37. We assume that alkylation of the NH functionality will not dramatically change the relative energy of the catalyst's TDI; therefore, the relative rate of hydride transfer could be approximated to be the relative rate of the catalytic reaction.

(46) Note that for this complex, in contrast to the fully methylated Noyori catalyst, the two hydrides are inequivalent and the substrate may approach both hydrides within the outer-sphere. The barrier for the outer-sphere hydride transfer *anti* to N(Alk) is computationally prohibitive. The origin of this is an additional substrate/ligand Ph-groups repulsion within the corresponding CSC.

(47) A possible reason for this is much less repulsion originating within the CSC of ethylated Ru-MACHO catalyst and *anti*-methyl (*R*)-lactate with respect to the fully methylated Noyori catalyst and acetophenone: indeed upon ethylation, the relative position of the *anti*-methyl (*R*)-lactate is almost unaffected (and the corresponding TS is stabilized by a C−H···O HBI between one C−H group of the ethyl substituent and the oxygen atom of the substrate); however, acetophenone is more significantly displaced within the fully methylated Noyori catalyst with respect to the initial geometry observed in the TS for the nonmethylated catalyst.

(48) (a) Lundgren, R. J.; Stradiotto, M. *Chem. - Eur. J.* **2008**, *14*, 10388. (b) Lundgren, R. J.; Rankin, M. A.; McDonald, R.; Schatte, G.; Stradiotto, M. *Angew. Chem.* **2007**, *119*, 4816.

(49) Leong, C. G.; Akotsi, O. M.; Ferguson, M. J.; Bergens, S. H. *Chem. Commun.* **2003**, 750.

(50) Abdur-Rashid, K.; Faatz, M.; Lough, A. J.; Morris, R. H. *J. Am. Chem. Soc.* **2001**, *123*, 7473.

(51) (a) Dub, P. A.; Scott, B. L.; Gordon, J. C. *Organometallics* **2015**, *34*, 4464. (b) Xie, J.-H.; Liu, X.-Y.; Xie, J.-B.; Wang, L.-X.; Zhou, Q.-L. *Angew. Chem., Int. Ed.* **2011**, *50*, 7329.

(52) Abdur-Rashid, K.; Clapham, S. E.; Hadzovic, A.; Harvey, J. N.; Lough, A. J.; Morris, R. H. *J. Am. Chem. Soc.* **2002**, *124*, 15104.

(53) Blaser, H.-U., Federsel, H.-J., Eds. *Asymmetric Catalysis On Industrial Scale: Challenges, Approaches, and Solutions*, 2nd ed.; Wiley-VCH Verlag GmbH & Co. KGaA: 2010.

(54) Dub, P. A.; Gordon, J. C. Patent WO2015191505A1; Los Alamos National Security, LLC, USA, 2015.

(55) (a) Blomenkemper, M.; Schroeder, H.; Pape, T.; Hahn, F. E. *Inorg. Chim. Acta* **2011**, *366*, 76. (b) Palmer, D. C.; Taylor, E. C. *J. Org. Chem.* **1986**, *51*, 846.

(56) Dub, P. A.; Scott, B. L.; Gordon, J. C. *Dalton Trans.* **2016**, *45*, 1560.

(57) (a) Eschweiler, W. *Ber. Dtsch. Chem. Ges.* **1905**, *38*, 880. (b) Clarke, H. T.; Gillespie, H. B.; Weisshaus, S. Z. *J. Am. Chem. Soc.* **1933**, *55*, 4571.

(58) We reported the identity of complex **Ir1** in a previous contribution (see ref 51a), but the details of its synthesis and characterization, including its X-ray structure, are reported for the first time in this work.

(59) (a) Xie, M.; Zhu, G.; Hu, Y.; Gu, H. *J. Phys. Chem. C* **2011**, *115*, 20596. (b) Capparelli, A. L.; Marañon, J.; Sorarrain, O. M.; Filgueria, R. R. *J. Mol. Struct.* **1974**, *23*, 145.

(60) The reaction also easily proceeds in other alcoholic solvents such as ^{i}PrOH, EtOH for both catalysts. However, the reaction is not a net hydrogenation (e.g., in ^{i}PrOH), since transfer hydrogenation also partially takes place as verified by separate experiments.

(61) Barrio, P.; Castarlenas, R.; Esteruelas, M. A.; Lledós, A.; Maseras, F.; Oñate, E.; Tomàs, J. *Organometallics* **2001**, *20*, 442.

(62) It is also interesting to note that both **Ir1** and **Ir2** seem to be much more efficient catalysts for the hydrogenation of **K7** than Noyori's catalyst, although in nonasymmetric fashion (see ref 63). For example, 1.46 g of **K7** is quantitatively hydrogenated with only 5.4×10^{-2} mg of **Ir1**.

(63) (a) de Koning, P. D.; Jackson, M.; Lennon, I. C. *Org. Process Res. Dev.* **2006**, *10*, 1054. (b) Ohkuma, T.; Koizumi, M.; Doucet, H.; Pham, T.; Kozawa, M.; Murata, K.; Katayama, E.; Yokozawa, T.; Ikariya, T.; Noyori, R. *J. Am. Chem. Soc.* **1998**, *120*, 13529.

(64) (a) Gladiali, S.; Alberico, E. *Chem. Soc. Rev.* **2006**, *35*, 226. (b) Bar, R.; Sasson, Y. *Tetrahedron Lett.* **1981**, *22*, 1709. (c) Heydrich, G.; Gralla, G.; Rauls, M.; Schmidt-Leithoff, J.; Ebel, K.; Krause, W.; Oehlenschlaeger, S.; Jaekel, C.; Friedrich, M.; Bergner, E. J.; Kashani-Shirazi, N.; Paciello, R. Patent WO2009068444A2; BASF SE, Germany, 2009.

(65) John, J. M.; Takebayashi, S.; Dabral, N.; Miskolzie, M.; Bergens, S. H. *J. Am. Chem. Soc.* **2013**, *135*, 8578.

(66) Kuze, N.; Ishikawa, A.; Kono, M.; Kobayashi, T.; Fuchisawa, N.; Tsuji, T.; Takeuchi, H. *J. Phys. Chem. A* **2015**, *119*, 1774.

(67) (a) Ramanjaneyulu, B. T.; Mahesh, S.; Vijaya Anand, R. *Org. Lett.* **2015**, *17*, 6. (b) Duncton, M. A. J.; Singh, R. *Org. Lett.* **2013**, *15*, 4284. (c) Tran, G.; Meier, R.; Harris, L.; Browne, D. L.; Ley, S. V. *J. Org. Chem.* **2012**, *77*, 11071. (d) Zhang, Y.; Zhang, X.; Xie, Y.; Huang, L. Patent CN102603646A; Zhejiang University: P. R. China, 2012. (e) Fritz, S. P.; West, T. H.; McGarrigle, E. M.; Aggarwal, V. K. *Org. Lett.* **2012**, *14*, 6370. (f) Borkin, D. A.; Landge, S. M.; Toeroek, B. *Chirality* **2011**, *23*, 612. (g) Prakash, G. K. S.; Paknia, F.; Mathew, T.; Mloston, G.; Joschek, J. P.; Olah, G. A. *Org. Lett.* **2011**, *13*, 4128. (h) Nie, J.; Li, X.-J.; Zheng, D.-H.; Zhang, F.-G.; Cui, S.; Ma, J.-A. *J. Fluorine Chem.* **2011**, *132*, 468. (i) Wen, L.; Shen, Q.; Lu, L. *Org. Lett.* **2010**, *12*, 4655. (j) Mimura, H.; Kawada, K.; Yamashita, T.; Sakamoto, T.; Kikugawa, Y. *J. Fluorine Chem.* **2010**, *131*, 477. (k) Cho, E. J.; Senecal, T. D.; Kinzel, T.; Zhang, Y.; Watson, D. A.; Buchwald, S. L. *Science* **2010**, *328*, 1679. (l) Gulevich, A. V.; Shpilevaya, I. V.; Nenajdenko, V. G. *Eur. J. Org. Chem.* **2009**, *2009*, 3801. (m) Gagosz, F.; Zard, Z. S. *Org. Synth.* **2007**, *84*, 32.

(68) (a) Wang, J.; Sánchez-Roselló, M.; Aceña, J. L.; del Pozo, C.; Sorochinsky, A. E.; Fustero, S.; Soloshonok, V. A.; Liu, H. *Chem. Rev.* **2014**, *114*, 2432. (b) Török, B.; Sood, A.; Bag, S.; Kulkarni, A.; Borkin, D.; Lawler, E.; Dasgupta, S.; Landge, S.; Abid, M.; Zhou, W.; Foster, M.; LeVine, H.; Török, M. *ChemMedChem* **2012**, *7*, 910. (c) Filler, R.; Saha, R. *Future Med. Chem.* **2009**, *1*, 1370. (d) Ojima, I. *Fluorine in Medicinal Chemistry and Chemical Biology*; John Wiley & Sons, Ltd: 2009. (e) Quirmbach, M.; Steiner, H. *Chim. Oggi* **2009**, *27*, 23. (f) Hagmann, W. K. *J. Med. Chem.* **2008**, *51*, 4359. (g) Purser, S.; Moore, P. R.; Swallow, S.; Gouverneur, V. *Chem. Soc. Rev.* **2008**, *37*, 320. (h) Müller, K.; Faeh, C.; Diederich, F. *Science* **2007**, *317*, 1881. (i) Yale, H. L. *J. Med. Pharm. Chem.* **1959**, *1*, 121.

(69) (a) *Fluorine and the Environment: Agrochemicals, Archaeology, Green Chemistry & Water*; Tressaud, A., Ed.; Elsevier: 2006. (b) Coe, B. J.; Glenwright, S. J. *Coord. Chem. Rev.* **2000**, *203*, 5.

(70) (a) Tomashenko, O. A.; Grushin, V. V. *Chem. Rev.* **2011**, *111*, 4475. (b) Yamada, S.; Morita, C. *J. Am. Chem. Soc.* **2002**, *124*, 8184.

(71) Chen, X.; Jia, W.; Guo, R.; Graham, T. W.; Gullons, M. A.; Abdur-Rashid, K. *Dalton Trans.* **2009**, 1407.

(72) Hayes, J. M.; Deydier, E.; Ujaque, G.; Lledós, A.; Malacea-Kabbara, R.; Manoury, E.; Vincendeau, S.; Poli, R. *ACS Catal.* **2015**, *5*, 4368.

(73) Although *anti*-**E2** is computed to be 7.45 kcal·mol^{-1} more stable then *syn*-**E2** (ΔG°_{298K}), both conformers were considered in the computational analysis.

(74) Fukui, K. *Acc. Chem. Res.* **1981**, *14*, 363.

(75) Further analysis of the catalytic cycle for this catalyst and its methylated analog reveal that hydride transfer (and not H−H bond cleavage) is the TDTS; see the next section.

(76) If X = Na, an additional Na···O interaction is present.

(77) Hartmann, R.; Chen, P. *Angew. Chem., Int. Ed.* **2001**, *40*, 3581.

(78) The activation barrier for the MEHT within the IrNNa complex is computed to be 2.4 kcal·mol^{-1} uphill versus the IrNH complex. In fact, the corresponding TS is stabilized by a N−Na···O interaction (there is no N−H···O interaction within the IrNH complex), but this effect does not sufficiently compensate for the unfavorable thermodynamics of the reaction IrNH + MeONa = IrNNa + MeOH (7.0 kcal·mol^{-1} on free energy scale). However, this

DOI: 10.1021/jacs.6b11666
J. Am. Chem. Soc. 2017, 139, 1245−1260

interaction partially compensates for this thermodynamics in the following step involving H−H bond cleavage, which proceeds almost isoenergetically with the IrNH analog.

(79) The results of this work were presented at the Gordon Research Conference (GRC) on Organometallic Chemistry (Newport, RI, July 12−17, 2015), Pacifichem 2015 (Honolulu, HI, December 15−20, 2015), and the GRC on Green Chemistry (Stowe, VT, July 31−August 5, 2016).

(80) Zhang, L.; Han, Z.; Zhao, X.; Wang, Z.; Ding, K. *Angew. Chem., Int. Ed.* **2015**, *54*, 6186.

(81) The formation of the reaction product can be explained based on two reactions that likely take place in the catalytic reaction pool: 1) HCO_2^- + $HN(CH_2CH_2)_2O$ = $HC(O)N(CH_2CH_2)_2O$ + OH^-; HCO_2H + $HN(CH_2CH_2)_2O$ = $HC(O)N(CH_2CH_2)_2O$ + H_2O. In any case, it is evident that hydride transfer from the catalyst to CO_2 is the first step of the catalytic cycle.

(82) (a) Meot-Ner, M. *Chem. Rev.* **2012**, *112*, PR22. (b) Perrin, C. L. *Acc. Chem. Res.* **2010**, *43*, 1550. (c) Desiraju, G. R. *Chem. Commun.* **2005**, 2995. (d) Steiner, T. In *Implications of Molecular and Materials Structure for New Technologies*; Howard, J. A. K., Allen, F. H., Shields, G. P., Eds.; Springer: Netherlands: Dordrecht, 1999; p 185. (e) Emsley, J. *Chem. Soc. Rev.* **1980**, *9*, 91.

(83) Desiraju, G. R. *Acc. Chem. Res.* **1996**, *29*, 441.

(84) Prakash and Olah described the transformation of CO_2 into methanol in the presence of a polyamine with the same Ru-MACHO catalyst (ref 85). However, for this transformation the methylation of the N−H functionality is reported to be detrimental.

(85) Kothandaraman, J.; Goeppert, A.; Czaun, M.; Olah, G. A.; Prakash, G. K. S. *J. Am. Chem. Soc.* **2016**, *138*, 778.

(86) Note also that, as was discussed in ref 45, extrapolation of the relative rate of hydride transfer to the relative rate of the catalytic reaction is just an approximation. The efficacy ot two catalytic reactions, assuming that both follow transition state theory and other approximations are valid, should be compared based on corresponding energetic spans [ref 38].

(87) Gridnev, I.; Dub, P. A. *Enantioselection in Asymmetric Catalysis*; CRC Press LLC: 2016.

DOI: 10.1021/jacs.6b11666
J. Am. Chem. Soc. 2017, 139, 1245−1260